DOE/ER/40321-9

ANNUAL PROGRESS REPORT

January 1992

Alice C. Mignerey

Department of Chemistry and Biochemistry
University of Maryland
College Park, MD 20742

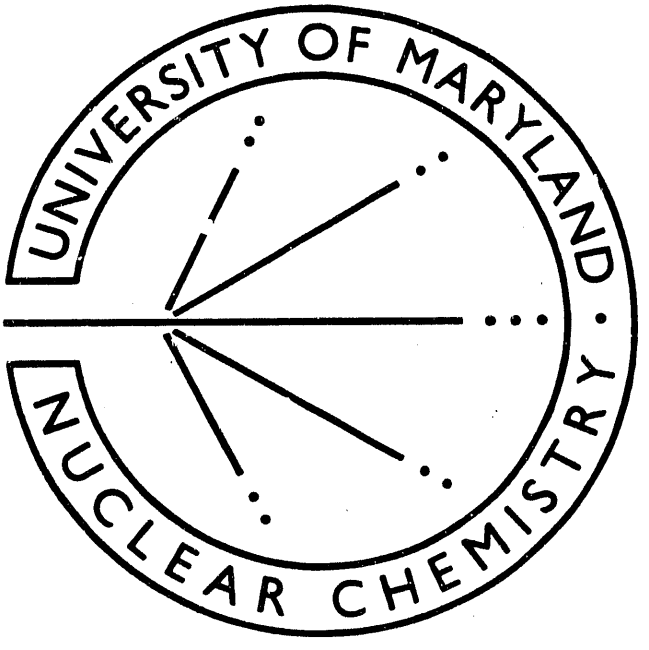

Work supported by the U. S. Department of Energy

Grant # DEFG05-87ER40321

DOE/ER/40321--9

DE92 008755

TABLE OF CONTENTS

I. Introduction

This report describes the activities of our research group for the period from January 1991 to January 1992. This past year saw my student Alfredo Marchetti complete his Ph.D. and officially graduate in December 1991. He has remained with the group while considering his career options and is concentrating on writing the scientific papers from his thesis research. The contribution in Section II.A is a brief summary of his results. Two other students Houria Madani and Bruce Libby have finished the bulk of their experimental data analysis and theoretical interpretation and are starting to write their theses. Each presented papers at the Eighth Nuclear Dynamics Workshop in Jackson Hole, January 18-24 1992. Copies of their contributions, which will be published in the conference proceedings, appear as Sections II.B and II.C.

A major advance in our research program came in September with the arrival of Jing Shea as a postdoctoral research associate with the group. She is a former student of Charlie Maguire from Vanderbilt and performed her thesis work at Oak Ridge National Laboratory working with Dan Shapira and his HILI detector. She designed and built a small fast plastic-CsI ring for her experiments there. She has worked very closely with our collaborators at Michigan State in designing the Very Forward Array to be used in experiments at the MSU National Superconducting Cyclotron, in conjunction with the MSU 4π Array. A description of the Very Forward Array and its capabilities can be found in Section II.D.

The group currently has two students who have just completed their coursework and are preparing for their qualifying exams. Edmundo Garcia-Solis has also been working on analyzing data taken by our group at the Oak Ridge HHIRF in November 1989. Daniel Russ spent last summer at the MSUNSCL familiarizing himself with the computer system there, in preparation for test runs this coming summer (1992) with the Very Forward Array. His thesis research will be based on experimental work with this and the MSU 4π Array.

This past fall probably marked the end of a long and fruitful program of experiments at the Bevalac. Bruce Libby and I participated in what will probably be the last Bevalac run for our group. With the likely impending closure of the Bevalac for nuclear science, our group has chosen

to move our intermediate energy program to MSU. This coincides with the ability of MSU to accelerate relatively massive beams to energies per nucleon greater than 50 MeV.

The research program has also started looking towards the long-term future and begun participation in activities related to the studies of ultrarelativistic heavy-ion reactions. Jing Shea and I attended the workshop on RHIC detectors held at Brookhaven in October 1991 and Jing went to Quark Matter '92. After careful consideration of the options and several group meetings, I made the decision to become a part of the PHOBOS collaboration, with Wit Busza from M.I.T. as the spokesperson. I hope that this will become a significant component of the research program.

II.A Comparison of Mass and Charge Distributions to Model Calculations in Cl-Induced Heavy-Ion Reactions

A.A. Marchetti, A.C. Mignerey, H. Madani, B. Libby, K. Morley†, W. Kehoe††, H. Breuer, and K. Wolf†††.

The results of the study of deep-inelastic reactions corresponding to the systems ^{37}Cl on ^{40}Ca and ^{209}Bi at E/A = 7.3 MeV, and ^{35}Cl on ^{209}Bi at E/A = 15 MeV are presented[1]. The projectile-like fragments were completely characterized in terms of mass, charge, and energy. Mass and charge distributions were determined for all three systems as a function of total kinetic energy loss (E_{loss}) in the N-Z plane. These distributions were characterized in terms of their centroids (<N> and <Z>), variances (σ_N^2 and σ_Z^2) and coefficients of correlation (ρ_{NZ}). Two methods were employed to determine these parameters: Gaussian fit and moment analysis. For the most part, no significant differences were found between the results of both methods, and, in the cases of disagreement, the meaning of the parameters is questionable.

The parameters of the experimental distributions were compared to two nucleon exchange models, one developed by J. Randrup[2] and the other developed by L. Tassan-Got[3]. It has been claimed[4] that the model recently developed by Tassan-Got seems to produce good estimates for the centroids. On the other hand, the centroids predicted by Randrup's model have shown large deviations from the experimental values in some cases. The primary distributions predicted by the models were fed to the evaporation code PACE II[5] to obtain the secondary distributions which were then compared to the experimental results. In the figures, the solid line represents Randrup's model calculations and the dashed line Tassan-Got's.

The values of <Z>, <N> and <N>/<Z> as a function of energy loss are shown in Fig. II.A.1 for the system ^{37}Cl + ^{40}Ca. The circles represent the experimental data. The <Z> and <N> decrease with increasing energy loss. The decrease in <N> is more or less a linear function. At 90 MeV of E_{loss}, <N> and <Z> have lost about 4.2 N units and 2.3 Z units, respectively. Mass deficits are observed at different values of E_{loss} that cannot be accounted by evaporation alone. For example, at 90 MeV of E_{loss} and assuming the excitation energy is divided equally, the amount of mass evaporated can be calculated to be around 4 mass units. Therefore, it appears that there should be a net flow of nucleons from the projectile to

the target to justify the mass deficit, unless, highly evaporative species are preferentially formed. The ratio <N>/<Z> initially decreases, as would be expected from a process of charge equilibration, and after about 40 MeV of energy loss remains more or less constant at a value of about 1.09. This ratio is very close to N/Z of the compound nucleus (1.08). There is a general good agreement between the model predictions of <Z>, <N>, and their ratio and the data.

In Fig. II.A.2 the values of σ_Z^2, σ_N^2, and ρ are displayed as a function of energy loss for the system $^{37}Cl + ^{40}Ca$. Both σ_Z^2 and σ_N^2 increase rapidly with E_{loss}. At 90 MeV of E_{loss}, the σ_Z^2 and σ_Z^2 reach values of around 20 and 30, respectively. The correlation coefficient increases sharply with energy loss and between 40 and 60 MeV reaches a more or less constant value very close to 1.0. The rapid increase of the variances and the correlation coefficient with energy loss occurs as the product distributions readily group around a diagonal line in the N-Z plane. It is clear that, as the energy loss increases, the experimental variances become substantially larger than the ones predicted by both models. This discrepancy occurs well before the entrance channel Coulomb barrier (E_{loss} ~ 93 MeV). The experimental correlation coefficient rises and tends to 1.0 faster than the model predictions.

The results of <Z>, <N>, and <N>/<Z> for the system $^{37}Cl + ^{209}Bi$ are shown in Fig. II.A.3. The circles and squares correspond to corrections of the energy loss scale assuming equal and thermal division of the excitation energy, respectively. For the most part, the differences between both corrections are not significant. However, after the first 20 MeV of energy loss, the <Z> and <N> corresponding to equal division of the excitation energy are increasingly smaller than those corresponding to thermal division. This result is expected, because evaporation increases with excitation energy, and, at a given energy loss, the equal division of excitation energy will deposit more excitation on the lighter partner than thermal division does. The <Z> and <N> decrease with increasing energy loss. At 70 MeV of E_{loss}, <N> and <Z> have lost about 1.6 N units and 1.0 Z units, respectively. The N centroid rises a little over 20 for the first 20 MeV of E_{loss}, while <Z> decreases steadily from 17. This seems to indicate a net transfer of neutrons from the target to the projectile and a net transfer of protons from the projectile to the target. Both <N> and <Z> behave rather linearly overall the entire E_{loss} range. The ratio <N>/<Z> rises slightly, and reaches a constant value immediately after about 20

MeV of energy loss. This value is around 1.24 and is far from the compound nucleus value 1.46.

Tassan-Got's model shows a good agreement in <Z> with the experimental data, while Randrup's model overestimates <Z>. For the first 40 MeV of energy loss, Tassan-Got's prediction of <N> is also good, after that value of energy loss, it slightly overpredicts <N>, but follows the trend of the experimental data. Randrup's model predicts an increase of <N> with increasing energy loss, even after evaporation corrections, a behavior opposite to the trend of the experimental data. There do not seem to be important differences in the ratio <N>/<Z> between the models and experiment for the first 40 MeV of energy loss. However, the experiment shows that this degree of freedom rises quickly and then remains more or less constant, while both models show a steady increase of the ratio with increasing energy loss.

The results of σ_Z^2, σ_N^2, and ρ are displayed as a function of energy loss for the system $^{37}Cl + ^{209}Bi$ in Fig. II.A.4. As in the previous case, both σ_Z^2 and σ_N^2 increase with energy loss but to a much lesser extend. At 70 MeV of E_{loss}, the variances in N and Z are about 5 and 2.5, respectively. These values are much lower than those observed with the ^{40}Ca target. A possible explanation is the contribution of fusion-fission products to the total width in the ^{40}Ca case. Such contribution should be absent from the projectile-like products in the deep-inelastic region for very asymmetric systems. The correlation coefficient raises sharply to a value around 0.4 in the first 20 MeV of energy loss. After that, it follows a smooth linear rise reaching a value of 0.7 at 70 MeV of E_{loss}. The grouping of the distributions along a diagonal line in the N-Z plane is not as dramatic as in the case of $^{37}Cl + ^{40}Ca$.

Randrup's model agrees very well with the experimental variances up to about 60 MeV of energy loss. Tassan-Got's model reproduces very well the Z variance, but it overestimates the N variance after the first 25 MeV of energy loss. The experimental correlation coefficient as a function of energy loss shows a sudden increase to a value of about 0.5, then a slow linear growth towards a value of 1.0. The models do not reproduce this behavior very well; they show an overall smooth increase of the coefficient with increasing energy loss.

The results of <Z>, <N>, and <Z>/<N> as a function of E_{loss} for the system $^{35}Cl + ^{209}Bi$ are shown in Fig. II.A.5. The circles and squares represent corrections of the energy loss scale corresponding to equal and thermal division of the excitation energy, respectively. There are no significant differences between

corrections for the first 100 MeV of E_{loss}. After that, the differences in <Z> start increasing with energy loss, reaching up to 2 Z units. The differences in <N> evolve similarly, giving differences of up to 4 N units. As expected, the <Z> and <N> corresponding to equal division of the excitation energy are smaller than those corresponding to thermal division. The value of <Z> decreases more or less steadily with increasing energy loss. At 100 MeV E_{loss}, <Z> has lost about 2 Z units. The value of <N> remains approximately constant (~ 18.5) up to about 100 MeV of E_{loss}, then it starts decreasing.

As in the case of $^{37}Cl + ^{209}Bi$, these results support a net flow of neutrons from the target to the projectile and of protons from the projectile to the target. However, the functional dependence of <N> shows a striking difference, which emphasizes the importance of N/Z in determining the product distributions. For the first 100 MeV of E_{loss}, <N>/<Z> increases up to about 1.25. Then it seems to start decreasing slowly, however, the fluctuations in the measured <N>/<Z> makes it difficult to establish this trend clearly.

Tassan-Got's model gives a better overall agreement with the experimental <Z> than does Randrup's model. However, both models fail to describe the evolution of the experimental <N> with energy loss. The ratio <N>/<Z> is underestimated by both models. It is interesting to note that while the experimental <N>/<Z> increases towards the composite system value (1.44) for the first 100 MeV of energy loss, both models predict a more or less constant value around 1.10. This is in contrast with the predictions for the system ^{37}Cl on ^{209}Bi.

For the system $^{35}Cl + ^{209}Bi$, the results of σ_Z^2, σ_N^2, and ρ are shown in Fig. II.A.6. Unfortunately, due to the experimental problems, the variances may have components that are not accounted for. These components may contribute mainly to the low energy loss portion of the spectra, since spurious contributions were observed in the mass coordinate around the elastic peak. These contributions should affect mainly σ_N^2 and ρ, and to a lesser degree σ_Z^2. This could explain the hump observed in σ_N^2 at 50 MeV of E_{loss}. However after 50 MeV of E_{loss}, the spectra are clean and it is possible to compare trends on the data with more confidence. The σ_Z^2 increases up to 100 MeV of energy loss, and from there on, starts decreasing. The σ_N^2 seems to follow more or less the same behavior. This is an interesting feature that is not observed in the other two systems. In the same energy region where the variances reach a maximum, there is a sudden change in the slope of the average values of N and Z as a function of energy loss. The correlation

coefficient shows a sudden increase at about 100 MeV of energy loss (going from negative to positive) and then remains approximately constant.

Both models predict a steady increase of the variances with energy loss. This is an interesting feature that is not observed in the other two systems. In the same energy region where the variances reach a maximum, there is a sudden change in the slope of the average values of N and Z as a function of energy loss. These findings seem to indicate that a different type of mechanism is starting to surface at higher energy losses. A breakup of the projectile-like fragment is a possible explanation for these observations; it would explain both the narrowing of the variances and the sudden negative drifts in <N> and <Z>. The experimental ρ is negative for the first 100 MeV of energy loss, in disagreement with both models, which predict a sudden rise followed by a smooth increase towards 1.0. However, it is not conclusive that there is anticorrelation, since the negative value could be the effect of the mass resolution.

It is interesting that two models that are very similar in their physical foundations predict such different trends for the mass and charge drift of asymmetric systems. According to Tassan-Got, the main difference between the two models is Randrup's use of the Lagrangian to derive the driving forces; the inclusion of kinetic terms in the potential (in particular rotational energy) that are not present in his description explains the discrepancy. D. Pal et al.[9] concluded that the inclusion of trajectory fluctuations in their calculations resulted in a much better agreement with the experiment than the use of the mean trajectory method (Randrup's model). It has also been suggested that the consideration of non-Markovian effects can also give a better description of the experimental data[10]. Overall, this stresses the need for a more realistic and quantitative description of the driving forces acting on the dinuclear system.

† presently at Indiana University
†† presently at M.I.T.
††† presently at Texas A&M

References

[1] A.A. Marchetti Ph.D. Thesis DOE-ER-40231-8
[2] J.Randrup, Nucl. Phys. A307,319 (1978); Nucl. Phys. A327,490 (1979);Nucl.

Phys. A382,468 (1982)
[3] L. Tassan-Got, Ph.D. Thesis INPO-T-89-02; Orsay, France 1988.
[4] A. Gavron, Phys. Rev. C21, 230 (1980)
[5] R. Planeta, et al., Phys. Rev. C38, 195 (1988)
[6] R. Planeta, et al., Phys. Rev. C41, 942 (1990)
[7] H. Breuer, et at., Phys. Rev. C28, 1080 (1983)
[8] D.K. Lock, et al., Phys. Rev. C31, 1268 (1985)
[9] D. Pal, et al., Phys. Rev. C41, 390 (1990)
[10] D. Pal, et al., Phys. Rev. G14, 1083 (1988)

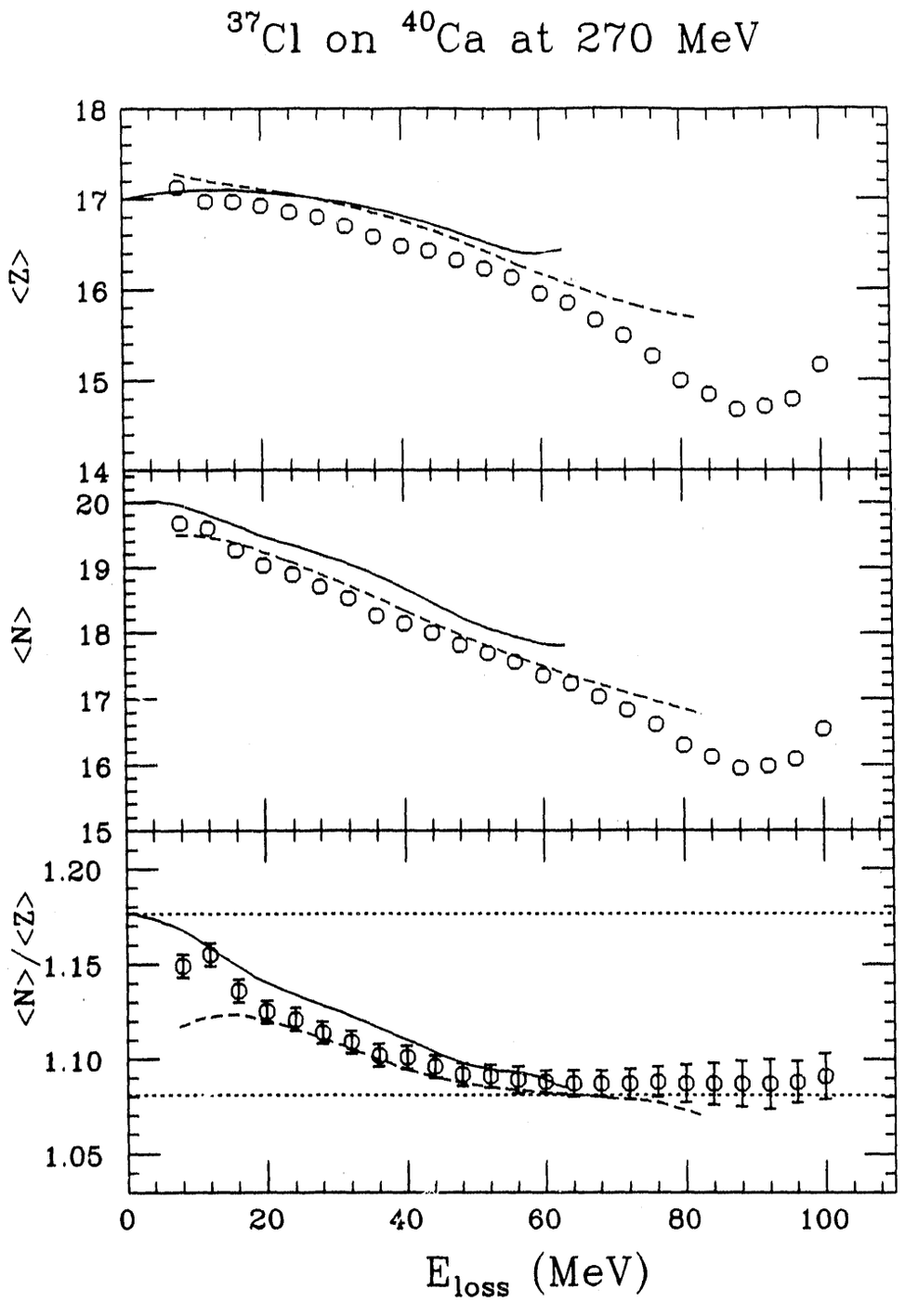

Figure II.A.1 Experimental results (circles) and model predictions for <Z>, <N>, and <N>/<Z> corresponding to the secondary distributions of the reaction ^{37}Cl on ^{40}Ca at 270 MeV as a function of energy loss. The solid line represents the results from Randrup's model and the dashed line represents the results from Tassan-Got's. The horizontal dotted lines represent the ratio N/Z of the projectile (top) and compound system (bottom), respectively.

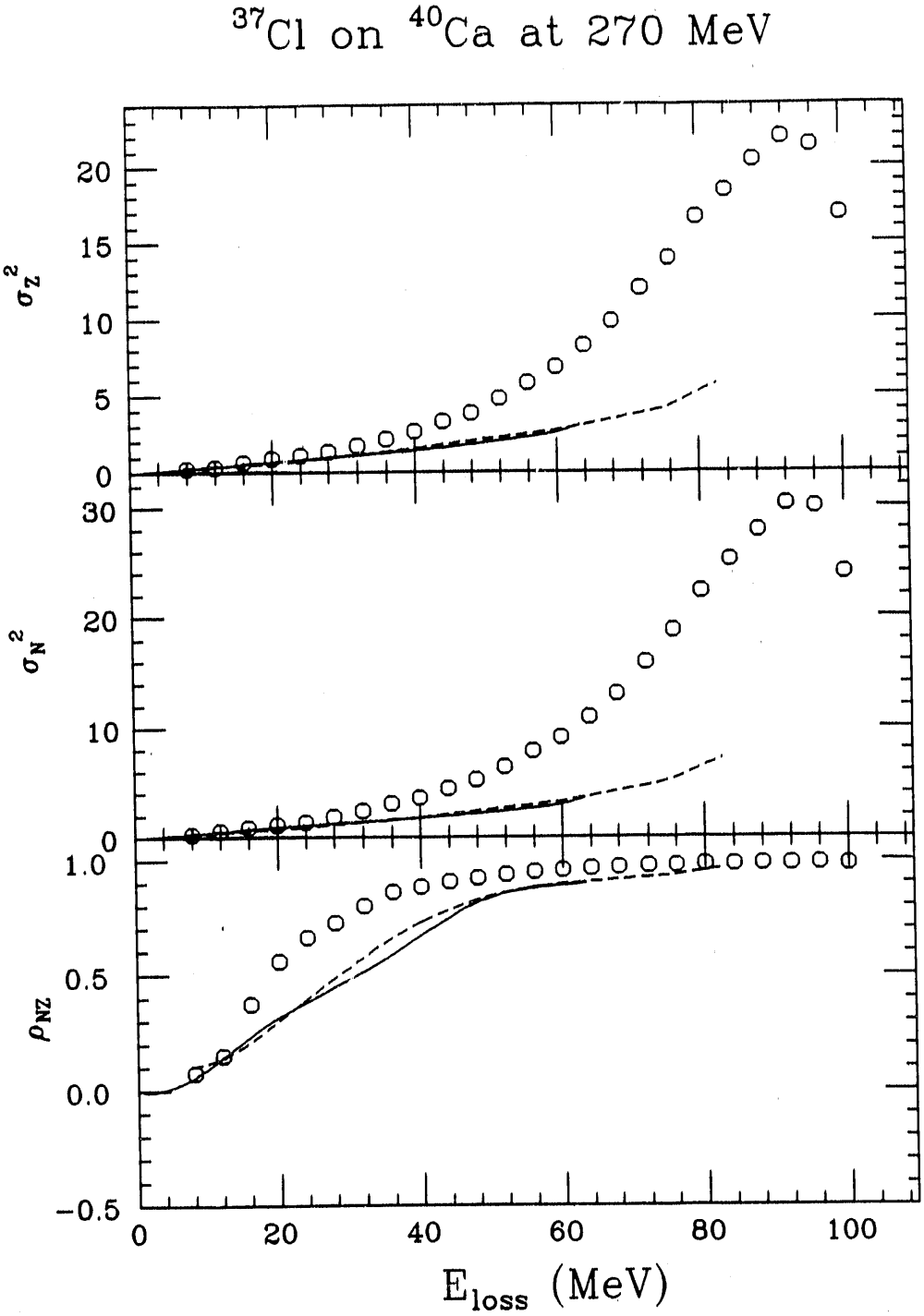

Figure II.A.2 Experimental results (circles) and model predictions for σ^2_Z, σ^2_N, and ρ_{NZ} corresponding to the secondary distributions of the reaction ^{37}Cl on ^{40}Ca at 270 MeV as a function of energy loss.The solid line represents the results from Randrup's model and the dashed line represents the results from Tassan-Got's.

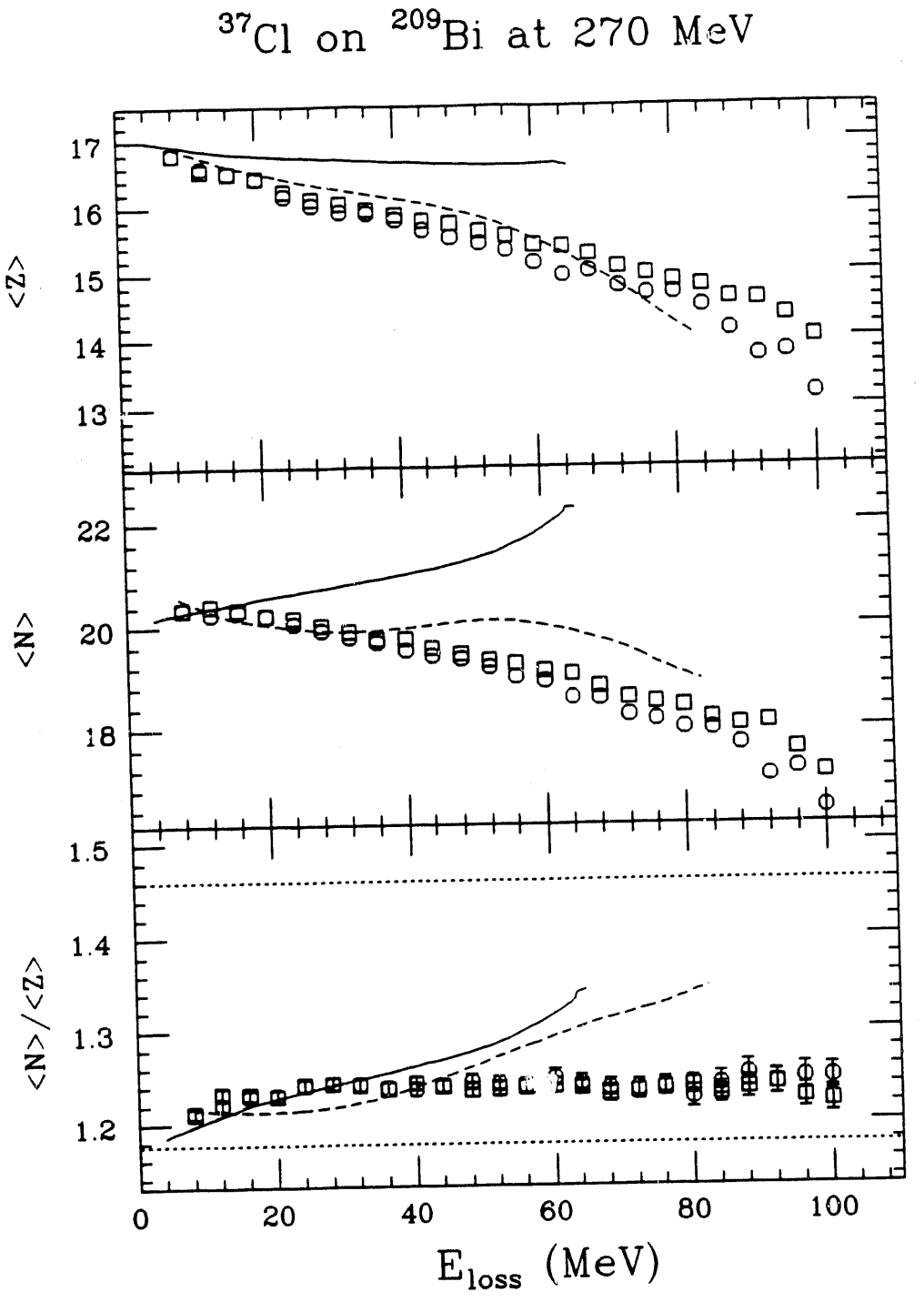

Figure II.A.3 Experimental results (circles and squares) and model predictions for <Z>, <N>, and <N>/<Z> corresponding to the secondary distributions of the reaction ^{37}Cl on ^{209}Bi at 270 MeV as a function of energy loss. The solid line represents the results from Randrup's model and the dashed line represents the results from Tassan-Got's. The circles and squares represent the results after correcting the energy loss scale assuming equal and thermal division of the excitation energy, respectively. The horizontal dotted lines represent the ratio N/Z of the projectile (bottom) and compound system (top), respectively.

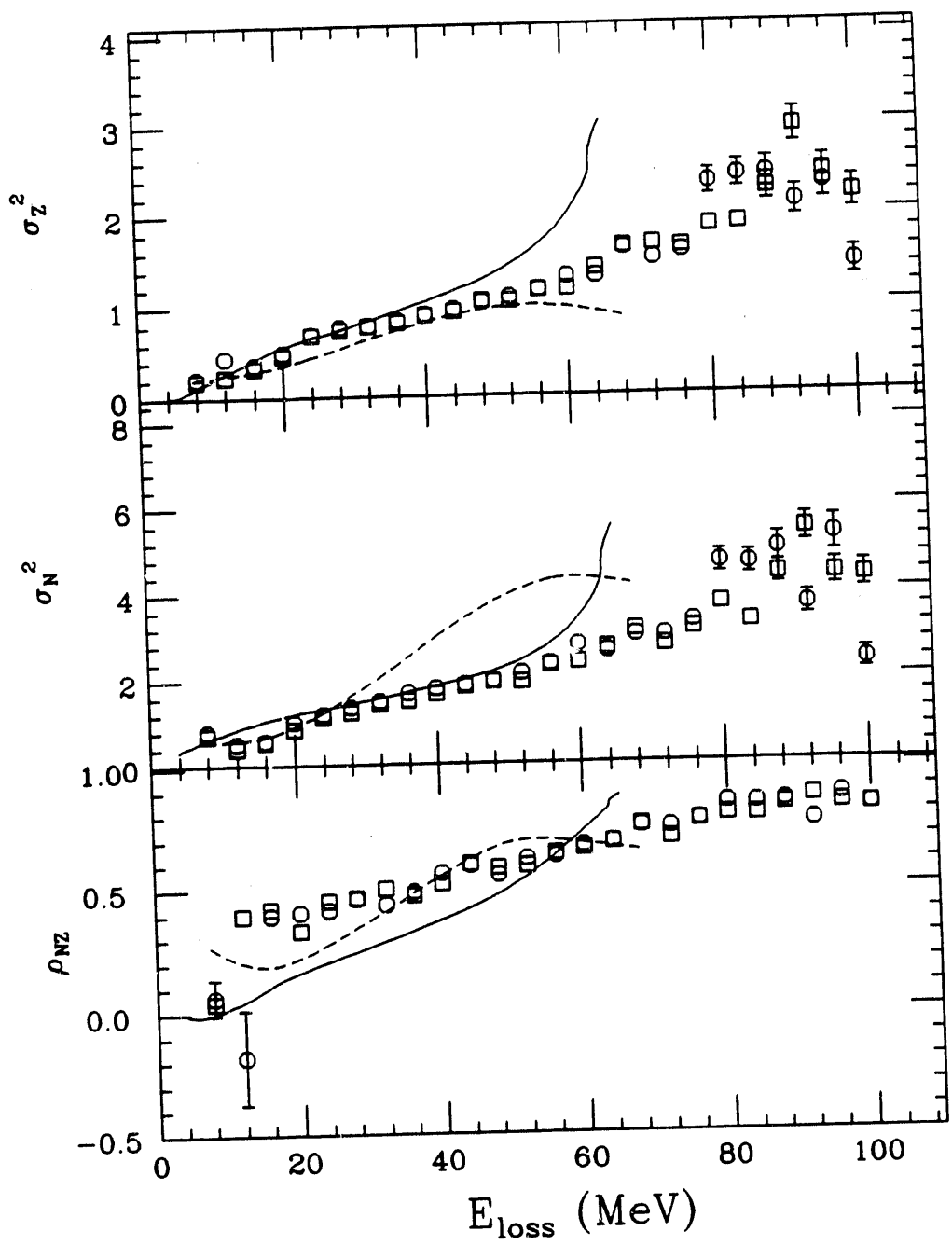

Figure II.A.4 Experimental results (circles and squares) and model predictions for σ^2_Z, σ^2_N, and ρ_{NZ} corresponding to the secondary distributions of the reaction ^{37}Cl on ^{209}Bi at 270 MeV as a function of energy loss. The solid line represents the results from Randrup's model and the dashed line represents the results from Tassan-Got's. The circles and squares represent the results after correcting the energy loss scale assuming equal and thermal division of the excitation energy, respectively.

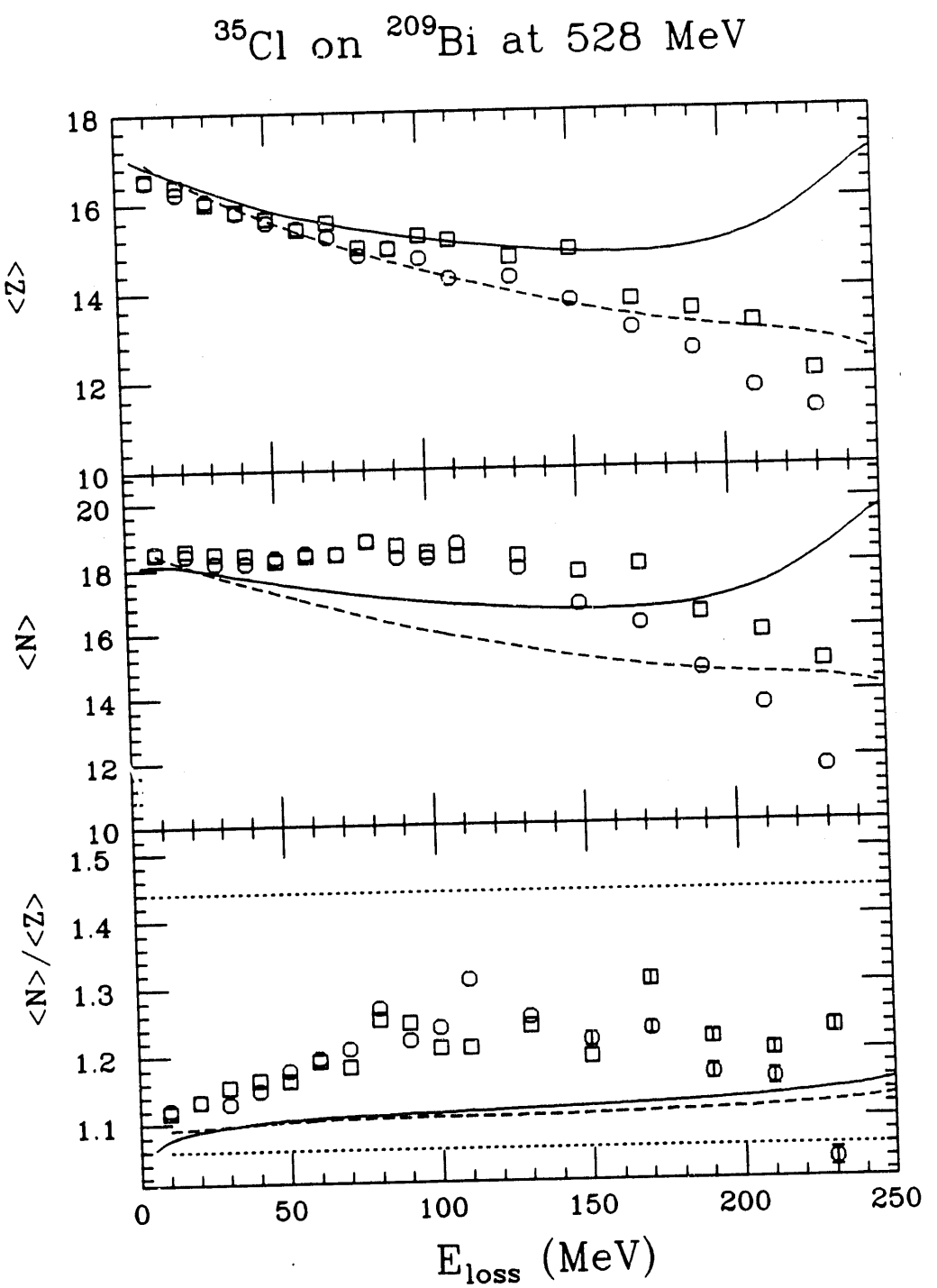

Figure II.A.5 Experimental results (circles and squares) and model predictions for <Z>, <N>, and <N>/<Z> corresponding to the secondary distributions of the reaction ^{35}Cl on ^{209}Bi at 528 MeV as a function of energy loss. The solid line represents the results from Randrup's model and the dashed line represents the results from Tassan-Got's. The circles and squares represent the results after correcting the energy loss scale assuming equal and thermal division of the excitation energy, respectively. The horizontal dotted lines represent the ratio N/Z of the projectile (bottom) and compound system (top), respectively.

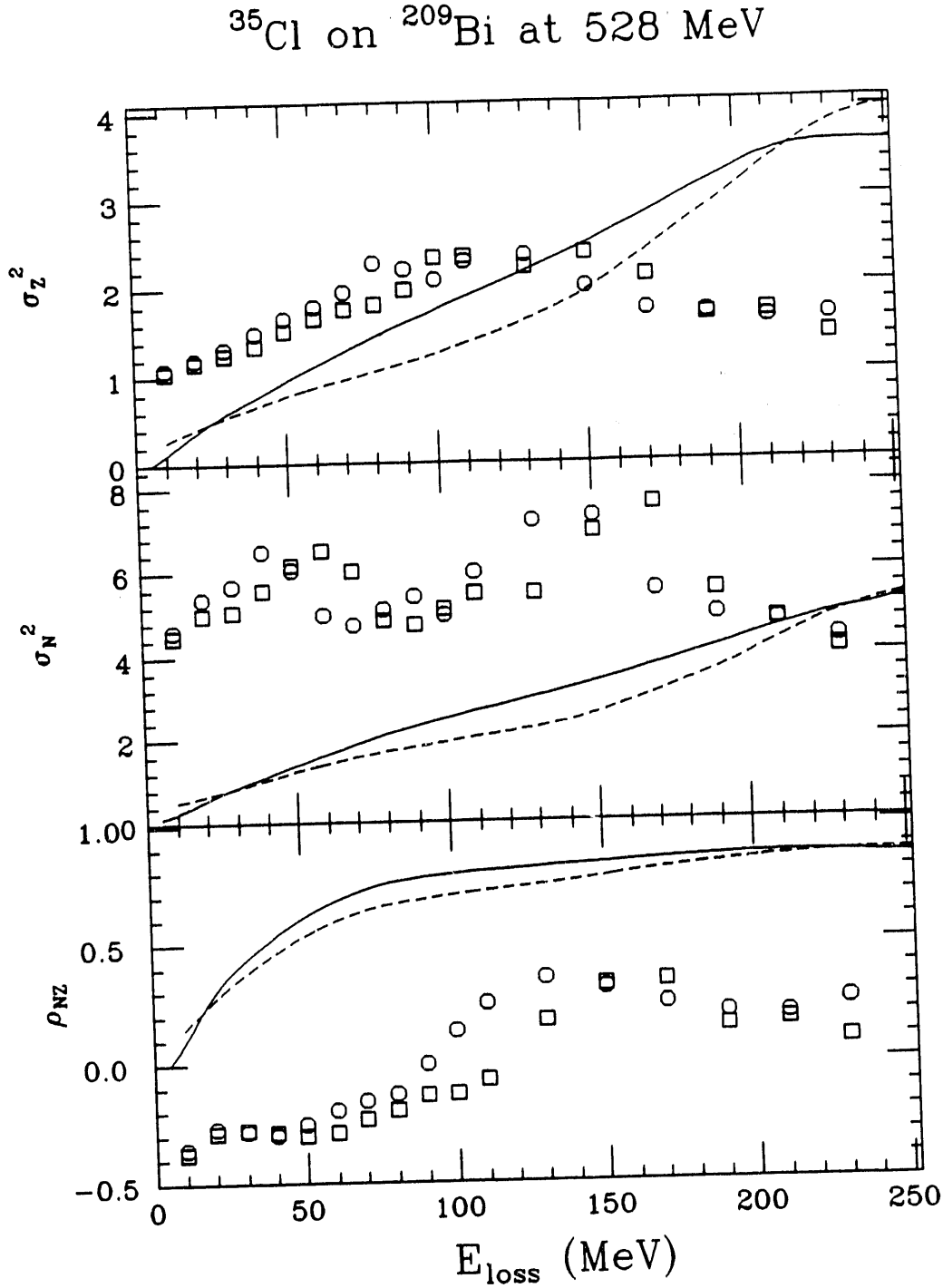

Figure II.A.6 Experimental results (circles and squares) and model predictions for σ^2_Z, σ^2_N, and ρ_{NZ} corresponding to the secondary distributions of the reaction ^{35}Cl on ^{209}Bi at 528 MeV as a function of energy loss. The solid line represents the results from Randrup's model and the dashed line represents the results from Tassan-Got's. The circles and squares represent the the results after correcting the energy loss scale assuming equal and thermal division of the excitation energy, respectively.

II.B COMPARISON OF MASS AND CHARGE DISTRIBUTIONS TO MODEL PREDICTIONS IN DEEP INELASTIC REACTIONS

H. MADANI, A.A. MARCHETTI, and A.C. MIGNEREY
Department of Chemistry, University of Maryland, College Park, Maryland 20742 USA

ABSTRACT

The mass and charge distributions of projectile-like fragments of heavy ion reactions at bombarding energies ranging from E/A = 8.5 MeV to 15 MeV are compared to the predictions of two nucleon exchange models. The drift towards mass asymmetry of asymmetric systems is fairly well reproduced by one of the models. The excitation energy produced in the ^{56}Fe on ^{165}Ho reaction at 672 MeV bombarding energy is shown to be equally divided between the two primary fragments. Only a very slight dependence of the projectile-like fragment excitation energy on its primary mass is observed.

Results from studies performed on heavy-ion reactions in the deep-inelastic region agree on some of the general features of these reactions. At low bombarding energies, the system remains binary and the two fragments emerging from the collision carry almost all the nucleons of the system. Memory of the entrance channel is retained. Relative kinetic energy is converted into excitation energy of the two fragments which then decay by particle evaporation and gamma emission or fission. The broadening of the mass and charge distributions with total kinetic energy loss indicates the presence of nucleon transfers between the fragments. However, it is not clearly understood yet if nucleon transfer alone can account for all the excitation energy produced and how this energy is divided between the two primary fragments. Another point to be elucidated is the strong drift towards mass asymmetry that is observed in many asymmetric systems. Ambiguous conclusions were drawn from results of experiments performed on different systems. The study of the 887-MeV ^{58}Ni on ^{197}Au by Awes *et al.*[1] resulted in an agreement between the data and the predictions of the potential energy surface (PES) gradient calculation only if equal excitation energy division between the two reaction partners is assumed. On the other hand, experiments with ^{58}Ni and ^{64}Ni on ^{238}U, ^{74}Ge on ^{165}Ho, and ^{56}Fe on ^{165}Ho at 8.3 MeV/u showed that the experimental data do not always follow the PES gradient predictions[2].

Several nucleon exchange models[3,4] have been developed to simulate the process of nucleon transfer and energy damping for deep-inelastic reactions at low and intermediate energies. Two extreme cases for excitation energy division are equal division,

and a division according to the two partners mass ratio, in this case the two primary fragments are in thermal equilibrium. Comparisons of model predictions to experimental data showed an equipartition of the excitation energy in some cases and a division according to mass in other cases[5,6]. Results from some of the most recent data agree with theoretical predictions where a smooth transition from equal division at low total kinetic energy loss to thermal equilibrium at higher total kinetic energy loss is exhibited[6,7]. These contradictory results lead to the conclusion that the models being used so far do not adequately describe the mechanisms of energy damping.

In the present contribution, data from the 505-MeV and 672-MeV ^{56}Fe on ^{165}Ho, and the 840-MeV ^{56}Fe on ^{56}Fe, and ^{56}Fe on ^{238}U reactions[8,9,10] are compared to predictions of one of the earliest nucleon exchange models, Randrup's model, and a relatively new model based on stochastic exchange of nucleons developed by Tassan-Got for higher bombarding energies. Both models follow the evolution of charge and neutron number centroids and their variances with total kinetic energy loss. distributions. In both models nucleon exchange is considered to be the sole contributor to energy dissipation. In Randrup's model, a mean trajectory approach, where the dynamical equations of motion are described by a Lagrange-Rayleigh equation, is used. On the other hand, in Tassan-Got's model, the statistical exchange of nucleons is simulated by a Monte Carlo process where the transfer of a nucleon one way or the other is decided by random drawing. More detailed descriptions of these models can be found in references 2 and 3. Only the differences that are thought to be pertinent to the discrepancies between the results of the two models will be discussed here.

In Randrup's model, the Fermi level gaps that govern the N and Z distributions are derived from a Lagrangian that contains a centrifugal term. It seems that it is the presence of this centrifugal term that leads the system to drift towards mass symmetry. In Tassan-Got's model, the Fermi levels are calculated from the energy separations of the corresponding nucleon, making the mass and charge drifts insensitive to the relative kinetic energy. Another characteristic of Tassan-Got's model is that only nucleons moving towards the window contribute to the energy damping. In Randrup's model, there is no restriction on the direction of transfer[3,4].

The primary Z and N centroids and their variances (σ_Z^2, σ_N^2), the N/Z ratio and the N-Z correlation factor (ρ_{NZ}) are plotted against the total kinetic energy loss in Figure II.B.1. for the 840-MeV ^{56}Fe on ^{56}Fe system. Both models agree in predicting the absence of Z and N drift in this symmetric system. The centroids and N/Z ratios predicted for the asymmetric systems 505-MeV and 672-MeV ^{56}Fe on ^{165}Ho, and 840-MeV ^{56}Fe on ^{238}U are shown in Figure II.B.2 The N/Z ratio is shown to be equally equilibrated in both calculations. However this result is obtained in two different ways. In Tassan-Got's model, the N/Z ratio equilibration is attained by means of proton transfer from the projectile-like fragment to the target-like fragment, and almost no neutron transfers. In Randrup's model, the N/Z equilibration is obtained by the transfer of neutrons from the target-like fragment to the projectile-like fragment. The transfer of protons

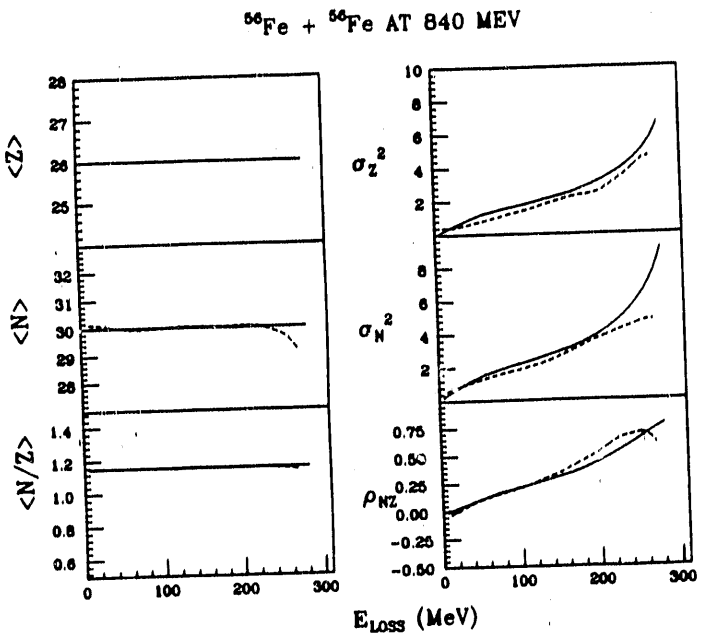

Figure II.B. 1: Theoretical primary distributions for the 840-MeV ^{56}Fe on ^{56}Fe system. The Solid and dashed lines are Randrup's model and Tassan-Got's model predictions, respectively.

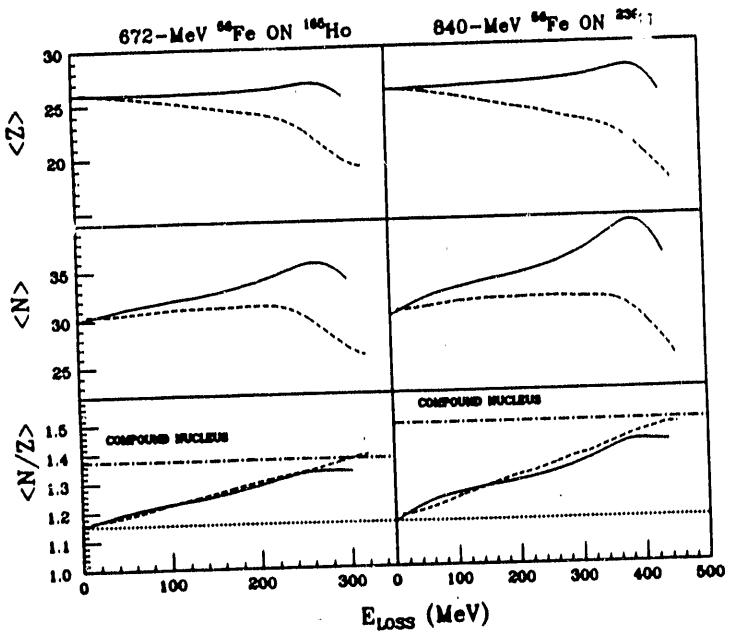

Figure II.B. 2: Theoretical primary distributions for the 672-MeV ^{56}Fe on ^{165}Ho and 840-MeV ^{56}Fe on ^{238}U systems. The Solid and dashed lines are Randrup's model and Tassan-Got's model predictions, respectively. The N/Z ratio of the projectile and the compound nucleus are indicated by the dotted lines and the dot-dashed lines respectiveley.

is negligible in this case. After evaporation corrections to the primary distributions obtained for each model, secondary distributions are obtained for the 505-MeV and 672-MeV ^{56}Fe on ^{165}Ho and 840-MeV ^{56}Fe on ^{238}U systems.

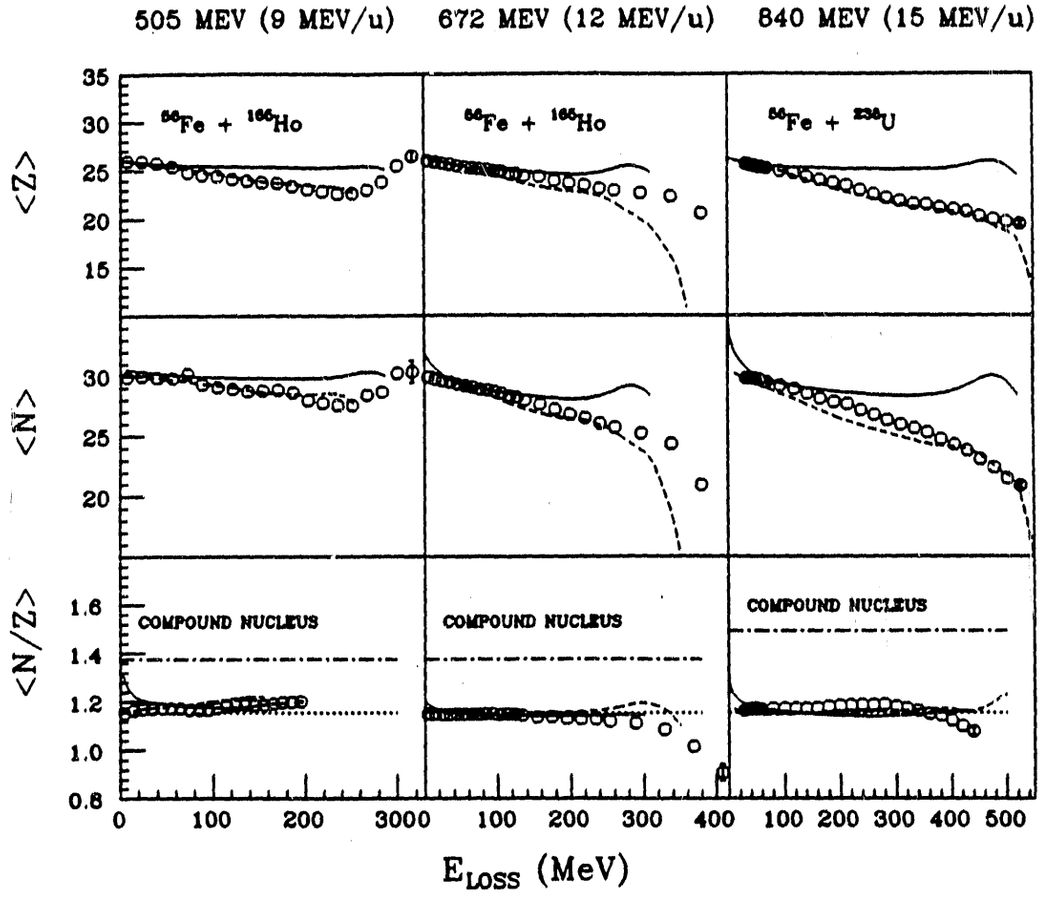

Figure II.B. 3: Comparison between experimental and theoretical secondary distributions for the 505-MeV and 672-MeV ^{56}Fe on ^{165}Ho and the 840-MeV ^{56}Fe on ^{238}U systems. The circles refer to the data points. The Solid and dashed lines are Randrup's model and Tassan-Got's model predictions, respectively. The N/Z ratio of the projectile and the compound nucleus are indicated by the dotted lines and the dot-dashed lines respectiveley.

The calculated N and Z centroids and the N/Z ratio for these three systems are compared to experimental data in Figure II.B.3. In all three cases, the N/Z equilibration is fairly well reproduced by both models. The experimental centroids agree with the predictions from Tassan-Got's model in all three cases. The centroids calculated from Randrup's model depart from the experimental data at an early stage of the reaction, especially for the higher bombarding energy and the more asymmetric system. The variances, which are not very sensitive to the driving forces, exhibit a

similar behavior for both models as shown in Figure II.B.4. The neutron variance, σ_N^2 is underpredicted by both models for the 672-MeV ^{56}Fe on ^{165}Ho system.

The nuclide distribution in the N-Z plane for the 672-MeV ^{56}Fe on ^{165}Ho and 840-MeV ^{56}Fe on ^{238}U systems displayed in Figure II.B.5, shows more drastically the discrepancy between the predictions of the two models and their description of the data. The experimental primary distributions were obtained by neutron evaporation

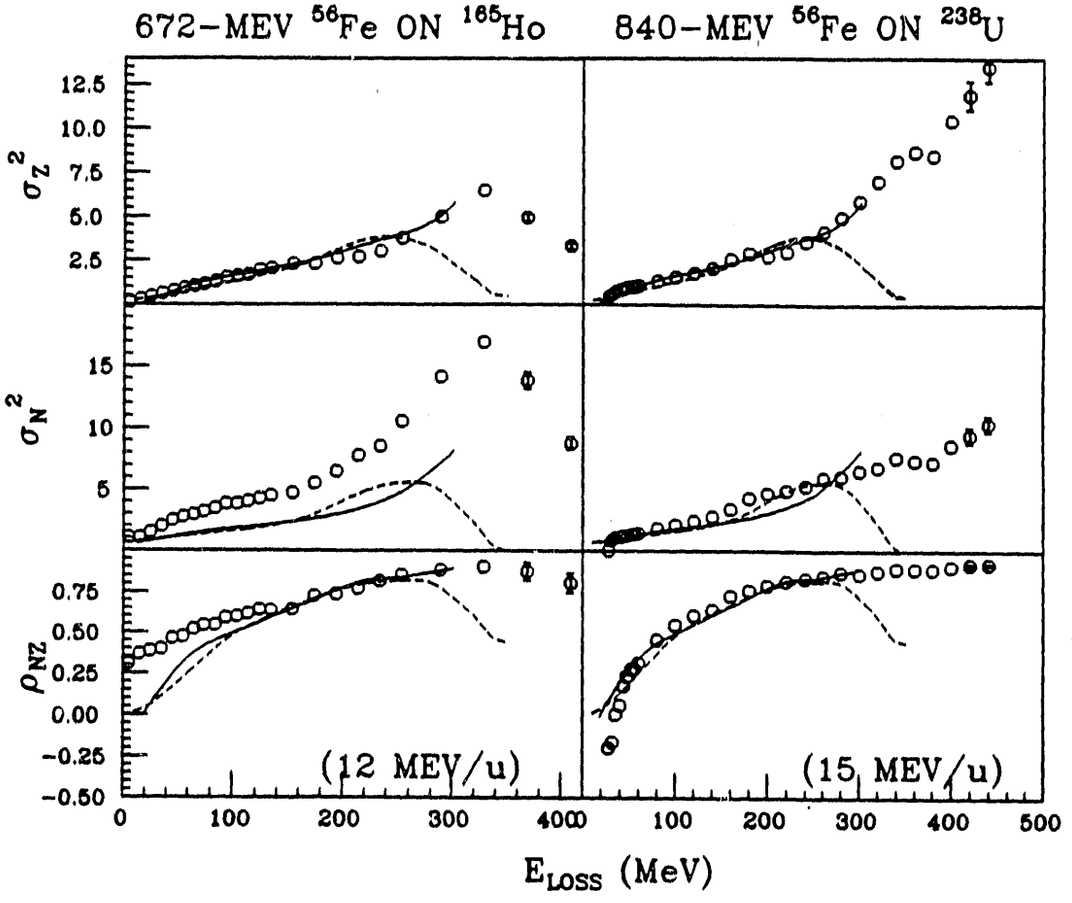

Figure II.B. 4: The variances σ_Z^2 and σ_N^2 and the correlation factor ρ_{NZ} for the 672-MeV ^{56}Fe on ^{165}Ho and the 840-MeV ^{56}Fe on ^{238}U systems. The circles refer to the data points. The Solid and dashed lines are Randrup's model and Tassan-Got's model predictions, respectively.

corrections for the 840-MeV ^{56}Fe on ^{238}U[10] system and by kinematic reconstruction from coincidence data for the 672-MeV ^{56}Fe on ^{165}Ho system. The gradient to the potential energy surface is represented by the arrow. Its direction predicts that the system should evolve towards mass symmetry. This is in accordance with the predictions of Randrup's model (solid curve). The data however exhibits a strong drift towards mass asymmetry and is fairly well reproduced by Tassan-Got's model

(dashed curve). This suggests that the N/Z equilibration in these asymmetric systems is achieved by proton transfer from projectile-like fragments to target-like fragments and virtually no neutron transfers. These results seem to support the idea that the N/Z equilibration is faster than mass equilibration.

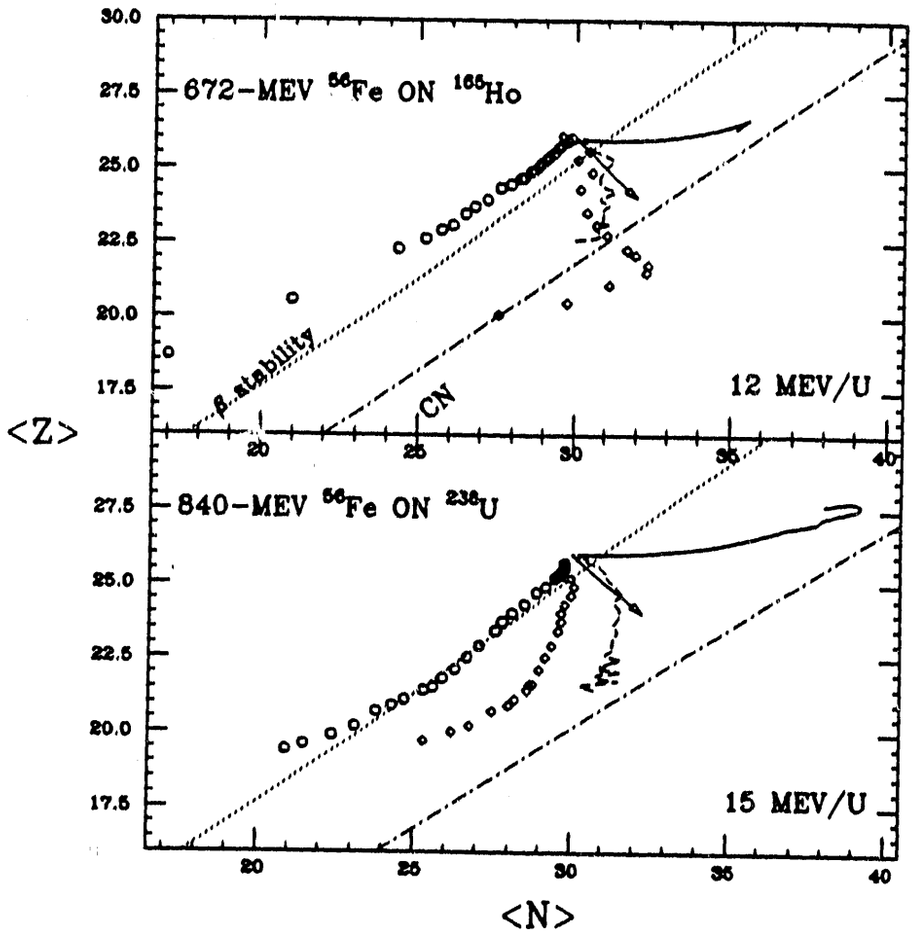

Figure II.B. 5: The nuclide distribution in the N-Z plane for the 672-MeV ^{56}Fe on ^{165}Ho and the 840-MeV ^{56}Fe on ^{238}U systems. The circles and diamonds refer to secondary data and reconstructed primary data respectively. The Solid and dashed lines are Randrup's model and Tassan-Got's model predictions, respectively. The arrow indicates the gradient to the PES at injection point. The beta stability line and the N/Z ratio of the compound nucleus are indicated by the dotted lines and the dot-dashed lines respectiveley.

The experimental primary mass of the projectile-like fragment produced by the 672-MeV ^{56}Fe on ^{165}Ho reaction was determined by two-body kinematic was then determined by use of the evaporation code PACE. In Figure II.B.6, the ratio of projectile-like fragment excitation energy to total excitation energy (E^*_{PLF}/E^*_{TOT}) of the system is plotted as a function of energy loss. The data seem to indicate that

the excitation energy is partitioned equally between the two primary fragments. At energy losses below 150 MeV, the E^*_{PLF}/E^*_{TOT} ratio is less than half. The predictions from the two models, displayed on the same plot, show an evolution of the system from an equipartition of the energy at low energy losses towards a thermal equilibrium at higher energy losses, although thermal equilibrium is not reached. Some studies[5,11,12] showed a dependence of the primary fragments excitation energy on their primary masses.

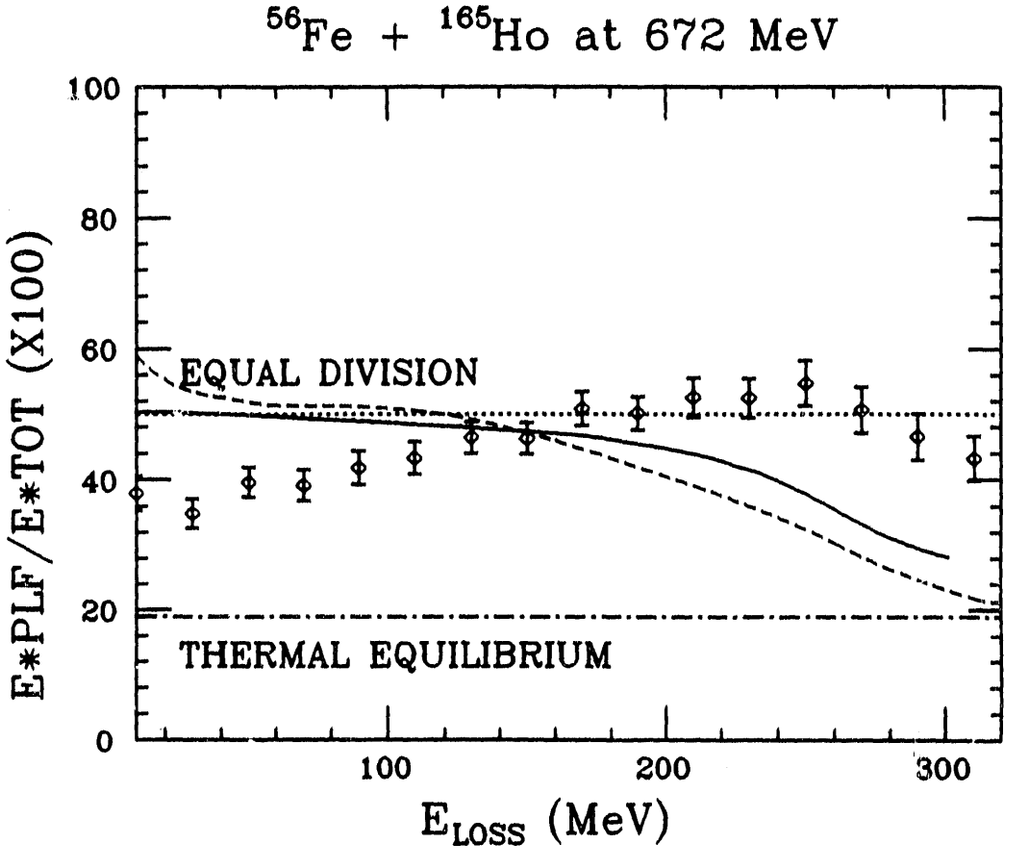

Figure II.B. 6: The PLF's fraction of excitation energy as a function of energy loss for the 672-MeV ^{56}Fe on ^{165}Ho system. The diamonds refer to the data points. The Solid and dashed lines are Randrup's model and Tassan-Got's model predictions, respectively. Equal excitation energy division and thermal equilibrium are indicated by the dotted lines and the dot-dashed lines respectiveley.

Plots of the E^*_{PLF} to E^*_{TOT} ratio versus primary projectile-like fragment mass for different energy loss bins are shown in Figure II.B.7. Only a very slight dependence is apparent inthe 672-MeV ^{56}Fe on ^{165}Ho system. Plotting the E^*_{PLF}/E^*_{TOT} ratio versus the energy loss for different primary projectile-like fragment mass gates in Figure II.B.8, confirms the fact that the excitation energy for the 672-MeV ^{56}Fe on ^{165}Ho

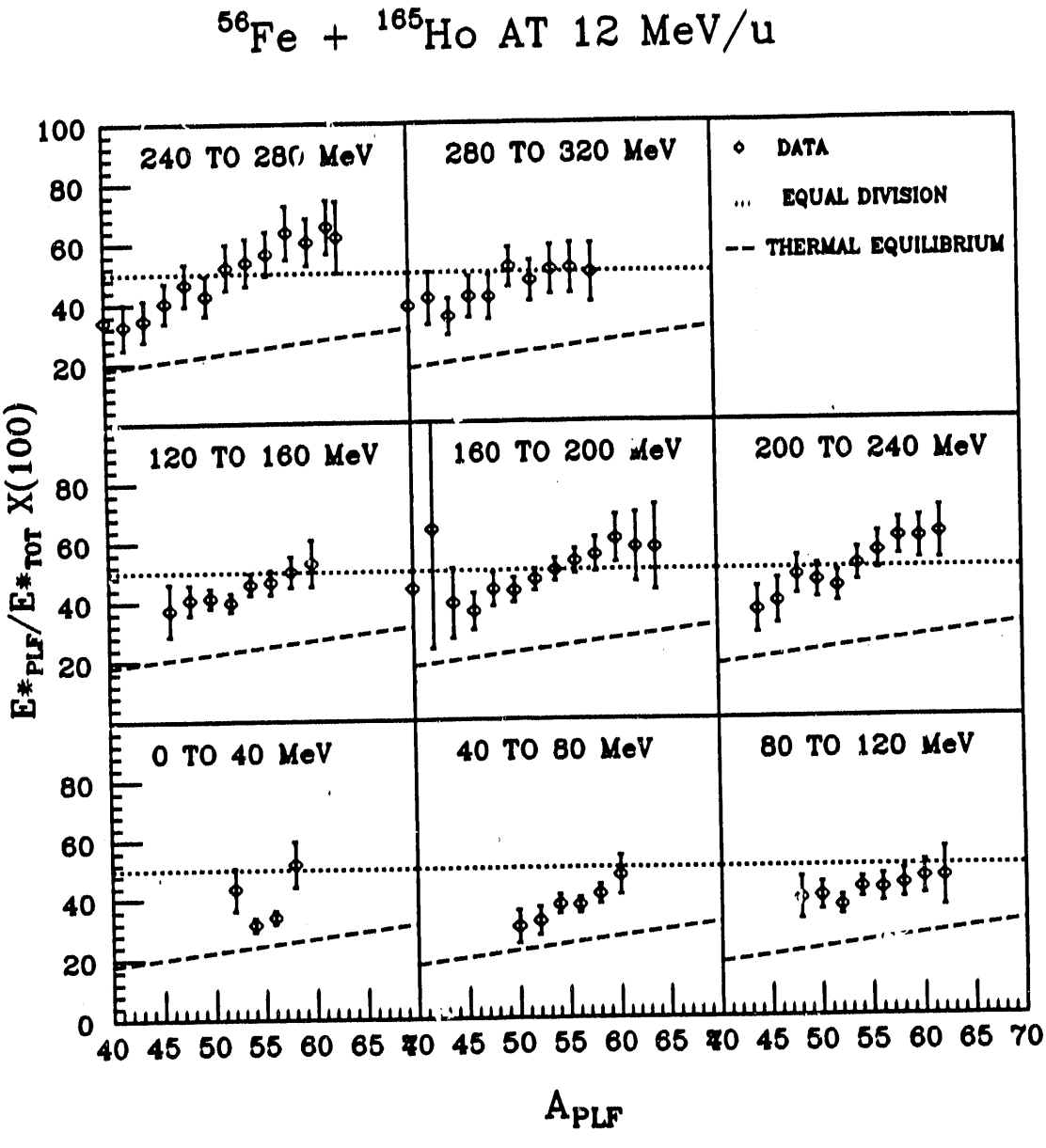

Figure II.B. 7: The PLF's fraction of excitation energy as a function of primary PLF mass for the 672-MeV ^{56}Fe on ^{165}Ho system, for different gates of energy loss . The diamonds refer to the data points. Equal excitation energy division and thermal equilibrium are indicated by the solid lines and the dashed lines respectiveley.

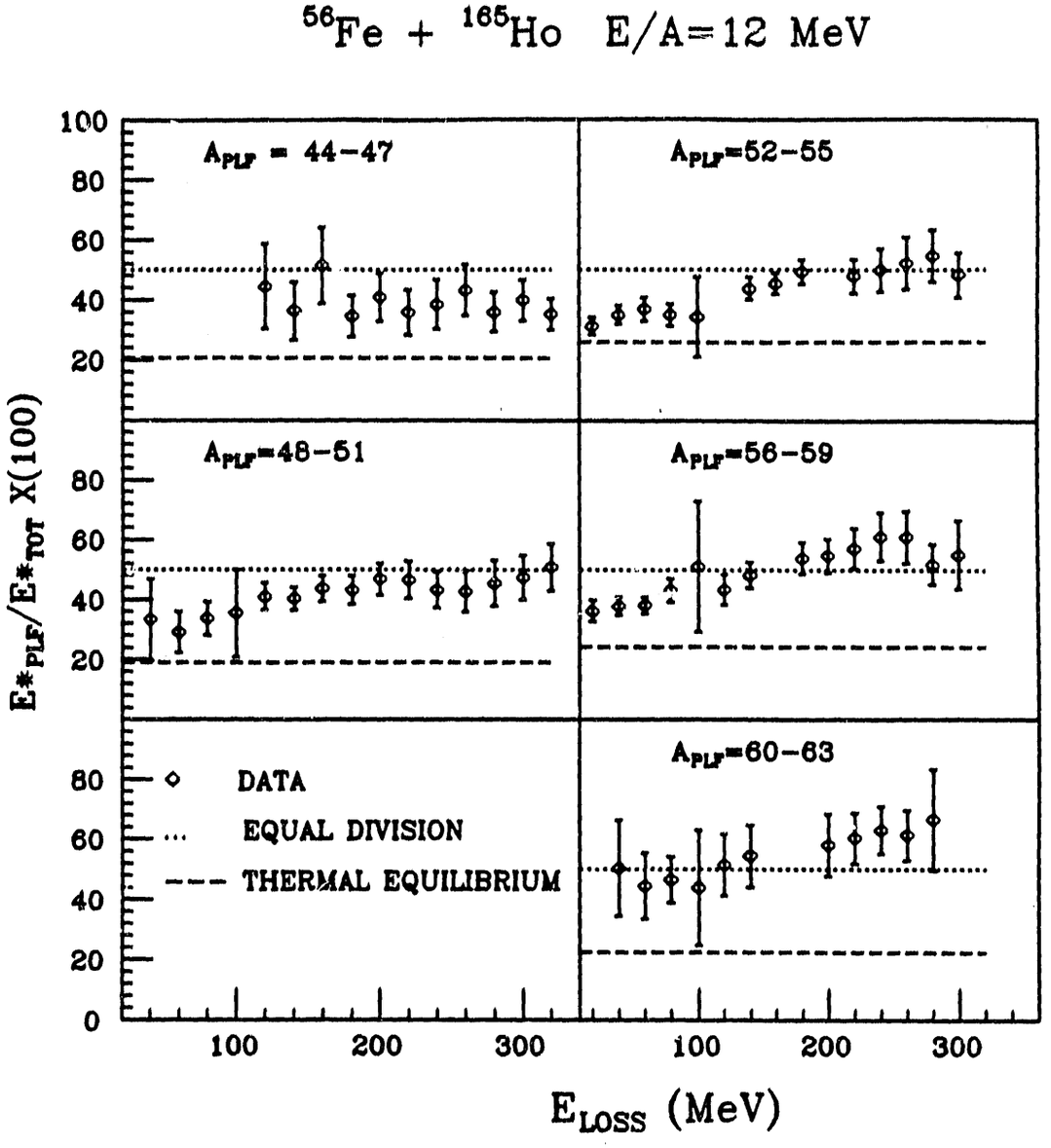

Figure II.B. 8: The PLF's fraction of excitation energy as a function of total kinetic energy loss for the 672-MeV ^{56}Fe on ^{165}Ho system, for different gates of primary PLF mass. The diamonds refer to the data points. Equal excitation energy division and thermal equilibrium are indicated by the solid lines and the dashed lines respectiveley.

system is divided equally between the two primary fragments and there is almost no dependence of excitation energy on primary fragment mass. What dependence there is may disappear when corrections are made due to mass resolutions. This was shown in studies using Pace simulations[13].

The generally good agreement between the predictions of Tassan-Got's model and the sets of data studied here suggest that nucleon transfers are sufficient to account for the energy damping in the deep-inelastic region of heavy-ion reactions at low bombarding energies. The N/Z equilibration seems to be reached faster than mass equilibration. This, along with the correlation between the N/Z ratio and proton drifts shown in a study of some systems by DeSouza *et al.*[14], could be an indication that the reason for the drift in asymmetric systems may be found in examining more closely N/Z asymmetries between projectile and target rather than mass asymmetries.

Acknowledgements

We wish to acknowledge the assistance of F. Obenshain in performing The 672-MeV ^{56}Fe on^{165}Ho experiment. The availability of the 840-MeV ^{56}Fe on ^{56}Fe and ^{56}Fe on ^{238}U data is courtesy of C. Merouane. We also wish to thank L. Tassan-Got for providing us with his stochastic transfer of nucleons code.

This work was supported by the U.S. Department of Energy, Office of Energy Research, Division of Nuclear Physics.

References

1. T.C. Awes, R.L Ferguson, R. Novotny, F. Obenshain, F. Plasil, S. Pontoppidan, V. Rauch, G. Young, and H. Sann, *Phys. Rev. Lett.* **52**, 251 (1984)
2. R. Planeta, K. Kwiatkowski, S.H. Zhou, V.E. Viola, H. Breuer, M.A. McMahan, W.L. Kehoe, and A.C. Mignery, *Phys. Rev.* **C41**, 942 (1990)
3. B. Borderie, M.F. Rivet, L. Tassan-Got, *Ann. Phys.* **15**, 287 (1990)
4. L. Tassan-Got, These de Doctorat d'Etat INPO-T-89-02; Orsay, France, 1988
5. D.R. Benton, Ph.D Thesis PP 86-030; University of Maryland, (1985)
6. D.R. Benton, H. Breuer, F. Khazaie, K. Kwiatkowski, V.E. Viola, S. Bradley, A.C. Mignerey, and A.P. Weston-Dawkes, *Phys. Rev.* **C38** 1207, (1988) *Phys. Lett.* **B185** 326, (1987)
7. V. Penumetcha, G.A. Petitt, T.C. Awes, J.R. Beene, R.L. Ferguson, F.E. Obenshain, F. Plasil, G.R. Young, S.P. Sorensen, *Phys. Rev.* **C42** 1480, (1990)
8. H. Breuer, N.R. Yoder, A.C. Mignerey, V.E. Viola, K. Kwiatkowski, K.L. Wolf, *Nucl. Instrum. Methods* **204**, 419 (1983)
9. H. Breuer, A.C. Mignerey, V.E. Viola, K.L. Wolf, J.R. Birkelund, D. Hilsher, J.R. Huizenga, W.U. Shroeder, W.W. Wilcke, *Phys. Rev.* **C28**, 1080 (1983)
10. C. Merouane, Ph.D. Thesis ORO-5172-0026; University of Maryland (1986)

11. K. Kwiatkowski, R. Planeta, S.H. Zhou, W.E. Viola, H. Breuer, M.A. McMahan, and A.C. Mignerey, *Phys. Rev.* **C41**, 958 (1990)
12. S. Chattopadhyay and D. Pal, *Phys. Rev.* **C42**, R2283 (1990)
13. J. Toke, W.U. Schroeder, J.R. Huizenga, *Phys. Rev.* **C40**, R1577 (1989)
14. R.T. De Souza, W.U. Schroder, J.R. Huizenga, R. Planeta, K. Kwiatkowski, V.E. Viola, and H. Breuer, *Phys. Rev.* **C40**, R1577 (1989)

II.C. THE DECAY OF HOT NUCLEI FORMED IN LA-INDUCED REACTIONS AT INTERMEDIATE ENERGIES

B. Libby, A.C. Mignerey, H. Madani, and A.A. Marchetti
Department of Chemistry, U. of Maryland, College Park, MD 20742

P. Roussel-Chomaz, N. Colonna, Y. Blumenfeld, G.F. Peaslee, D.N. Delis, M.A. McMahan, J.C. Meng, X. Sui, L.G. Moretto, and G.J. Wozniak
Lawrence Berkeley Laboratory

M. Colonna and M. DiToro
INFN Catania

ABSTRACT

The decay of hot nuclei formed in lanthanum-induced reactions utilizing inverse kinematics has been studied from E/A= 35 to 55 MeV. At each bombarding energy studied, the probability for the multiple emission of complex fragments has been found to be independent of target. Global features (total charge, source velocity) of the reaction La + Al at E/A = 45 MeV have been reproduced by coupling a dynamical model to study the collision stage of the reaction to a statistical model of nuclear decay.

Over the past several years the mechanism of the decay of hot nuclei formed in heavy ion reactions, and specifically the mechanism responsible for the emission of complex fragments (Z greater than 3), has been studied quite extensively. Many models have been proposed (the sequential binary decay of a compound nucleus[1], fragment formation due to dynamical instabilities in an expanding compound nucleus[2], the prompt multifragmentation of a hot system[3]) to interpret the experimental data. In some cases[4,5], different models arrive at similar conclusions, further muddying the picture. In an attempt to determine which mechanism(s) may be responsible for the emission of complex fragments, the inverse kinematics reactions La + C, Al, V or Ti, and Cu or Ni have been studied at bombarding energies of 35, 40, 45, and 55 MeV/u[6]. This provided an energy range of over 2 GeV in total available energy with which to study complex fragment emisssion. Coincident detection of up to five complex fragments for the heavier systems studied at the highest bombarding energy was accomplished by using a Si-Si(Li)-plastic array[7] in the side-by-side configuration.

The Z1-Z2 correlations for the systems studied over the entire range of bombarding energies are shown in Figure II.C.1. The reaction La+C is essentially binary, as indicated by a ridge at constant Z1+Z2. This binary ridge is present for the reactions

on Al until E/A=45 MeV, but with a significant amount of higher fold events signified by the increasing presence of contours below the Z1+Z2 ridge. The heavier targets lack a binary ridge for all energies. This arises from the increased importance of events of higher complex fragment multiplicity in which the event was not completely detected.

In order to further illustrate the Z1-Z2 correlations, the source velocity (defined as $\Sigma p(i)/m(i)$, in which p is the momentum of the fragment and m is its mass) is plotted as a function of the total charge detected in binary events for the reacting system, as shown in Figure II.C.2. The arrows are at the charge of the projectile, the numbers refer to the center-of-mass energy of the projectile, and the lines are at the complete fusion source velocity. The distributions are at a central value of total charge and source velocity for the reactions on C at a source velocity intermediate between the velocity of the beam and the compound nucleus velocity. This is a good indication that these systems undergo the binary decay of a compound nucleus formed in incomplete fusion reactions. As the bombarding energy or the mass of the target increases, the distribution broadens, indicating the lack of a well defined source for 2-fold events. The broadening of both the source velocity and the total Z distributions for these systems shows the increasing importance of decay by the emission of three or more complex fragments.

The source velocity distributions for events in which 2, 3, and 4 complex fragments were detected in the reactions at E/A=45 MeV are shown in Figure II.C.3. The shift to lower source velocity as the number of complex fragments increases indicates that more central collisions are needed to produce the higher fold events. The widths of the distributions arise from two processes- the evaporation of light particles and the different sources caused by reactions at different impact parameters. It has been estimated[6] that about half of the width in the reaction on Al is due to light particle evaporation, and this contribution decreases for the heavier targets. In other words, one can focus on reactions at different impact parameters by cutting the data at different source velocities. The probability of decaying by n-complex fragments (n=2,3,4,...) was determined in this manner, as shown in Figure II.C.4. The probability is relatively independent of the system being studied and dependent only on the source velocity. In order to remove the beam energy dependence from Figure II.C.4, the source velocity was transformed to excitation energy ($E^* = (As-Ap/As)Eb$, in which As is the source size determined from the source velocity, Ap is the mass of the projectile, and Eb is the bombarding energy in MeV) for each energy and system studied and the probabilities of decaying by an n-fold event were determined. As shown in Figure II.C.5, the probability of decaying by an n-fold event is relatively independent of both the system being studied and the bombarding energy and is dependent only on the excitation energy of the system.[6] Another important feature in Figure II.C.5 is that the decay probability of the higher multiplicity events shows only a gradual increase as the excitation energy increases past 5 MeV/u. This is at odds with several multifragmentation models, which predict a sharp increase in the

probability of decaying by higher fold events in this region of excitation energy.

In order to examine processes that could lead to complex fragment emission, the system La+Al at E/A=45 MeV has been studied by coupling a model that simulates the dynamical evolution of the system during the collision stage with a statistical decay model.

The dynamical evolution of the system was simulated by solving the Landau-Vlasov (or Boltzmann-Nordheim-Vlasov) equation with a test particle approach[8], in which a nucleon was represented by 40 test particles. The Landau-Vlasov equation combines a term representing the mean fields of the colliding nuclei with a collision term for nucleon-nucleon collisions. The mean field includes the Coulomb potential and a nuclear potential approximated by a density dependent Skyrme interaction. A compressibility constant of 200 MeV was used. The collision term included the free nucleon cross section with its energy and angular dependence. The dynamical evolution of the system was followed until the "freeze-out" time, the time at which pre-equilibrium emission of light particles has stopped and evaporation has begun. At the freeze-out time, a clusterization procedure is used to determine the properties (Z, A, excitation energy, and angular momentum) of the fragment or fragments present and these properties are then parameterized as inputs to the GEMINI statistical decay code.[1] At the freeze-out time, it may not be clear whether more than one fragment is present, so the dynamics are followed to longer times and the properties are extrapolated back to the freeze-out time.

In order to determine the freeze-out time, the mean energy of the light particles (protons and neutrons) is plotted as a function of time, as shown in Figure II.C.6, for central collisions. At larger impact parameters, there may be more than one fragment present so the source of the light particles may not be well defined. One of the sources may be close to equilibrium while the other may be far from it. Therefore, the properties of the fragments far from equilibrium will not be correctly determined for input into GEMINI. The mean energy of the light particles decreases until time= 90 fm/c, after which the energy is nearly constant. It is this change in the mean energy that is used to signal the change from pre-equilibrium to equilibrium emission.

The time evolution in space of the reacting system at E/A=45 MeV is shown in Figure II.C.7 for a range of impact parameters. For the most central collisions (b= 1,2 fm), a hot deformed system is formed, while at larger impact parameters (b= 5,6,7 fm), the mechanism is more reminiscent of deep inelastic collisions. For the intermediate impact parameters, the picture is less clear. While at first view it seems as though the system at b=3 fm also forms a hot system (as in the more central collisions), if density plots of nucleons in source are examined for times greater than 100 fm/c, as shown in Figure II.C.8, two centers of density can clearly be seen. This could be an indication of a fast fission type of mechanism could be present at E/A=45 MeV. This is consistent with fast fission systematics in the region of mass and excitation energy[9]. Also the fission barrier for this system has been calculated to disappear at entrance

l-waves at an impact parameter between 2 and 3 fm. Similar results are also obtained for the reacting system at b=4 fm. In order to determine whether invoking a fast fission mechanism helps reproduce experimental observables, the cross section was determined by parameterizing the GEMINI inputs both by considering the reaction product for b=3 and 4 fm to be a single fused system (without fast fission) and by cutting in space between the centers of density and back extrapolating the properties of the products to the freeze-out time.

Figure II.C.9 shows the cross section σ(Z) determined experimentally and by each of the methods described above. As is readily apparent, the scenario in which no fast fission mechanism is invoked vastly underpredicts the cross section for Z less than 20. The fast fission scenario slightly predicts the cross section in this region, but reproduces the general shape of the distribution. Also,the scenario without fast fission fails to predict decays in which three complex fragments are produced.

Figure II.C.10 shows the total charge detected and the source velocity ditributions determined experimentally (solid line) and from the model after the data was filtered through the detector geometry (dashed line). For the total charge detected, the peak for the model and for the data for 2-fold events are well matched, with the model slightly overpredicting the total charge for the n=3 events. In each case, the low total charge tail is not reproduced, which could come from underestimating the number of higher fold events in which not all fragments were detected. The peaks in the source velocity distributions are well reproduced by the model, but the widths of the distribution are narrower than for the experimental data.

Another way of interpreting the n=3 multiplicity data is to examine a Dalitz-like plot of the fragment Z distribution. In this kind of plot, three variables are plotted against each other, with the scales running from the edge to a vertex in a triangle. In this case, the scales are the ratio of the charge of one fragment to to total charge in an n=3 event. Shown in Figure II.C.11 are the experimental and model Dalitz-like plots. Although there is qualitative agreement between the experiment and the model, the model seems to underpredict the symmetric splits (shown as yield in the center of the Dalitz-like plot). Because the properties of the source of complex fragments (charge and source velocity) have been well reproduced by the model, the underprediction of the symmetric splits could arise from a failure to correctly calculate the fission barriers in this region of mass.

The study of the decay of hot nuclei formed in these La-induced reactions shows some striking features. Over a range of systems and bombarding energies the probability of decay by an event on n-complex fragments has been shown to be dependent only on the excitation energy of the system. The modelling of the reaction La+Al at E/A=45 MeV by combining a dynamical model to follow the collision stage of the reaction with a statistical model to follow the decay stage has reproduced global features of the reaction (source charge and velocity,cross sections) but fails to reproduce finer features, such as the more symmetric splits (shown as lack of yield in the center of Dalitz-like plots). Further work needs to be done to model the more symmetric

reactions and the more symmetric decay channels.

ACKNOWLEDGEMENTS: This work was supported by the U.S. Department of Energy, Division of Nuclear Physics of the Office of High Energy and Nuclear Physics.

REFERENCES:

1. Charity, R.J., et al, Nucl. Phys. A483(1988) 371
2. Bowman, D.R., et al, Phys. Rev. Let. 67(1991) 1527
3. Xiao-ze, Z., et al, Nucl. Phys. A461(1987) 668
4. Bowman, D.R., et al, Nucl. Phys. A523(1991) 386
5. Gross, D.H.E. Phys. Let. 203B(1988) 26
6. Blumenfeld, Y., et al, Phys. Rev. Let. 66(1991)576
7. Kehoe, W.L., et al NIM A311(1992) 258
8. Bonasera, A., et al, Phys. Let. 221B(1989) 233
Bonasera, A., et al, Phys. Let. 246B(1990) 337
9. Hinde, D.J., et al, Nucl. Phys. A502(1989) 497c

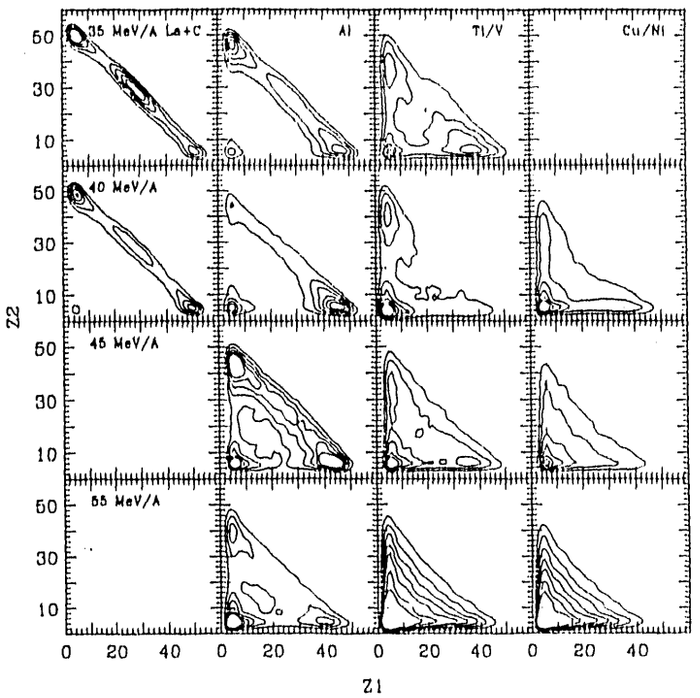

Figure II.C. 1: Z1-Z2 correlations for binary events for all systems and energies studied.

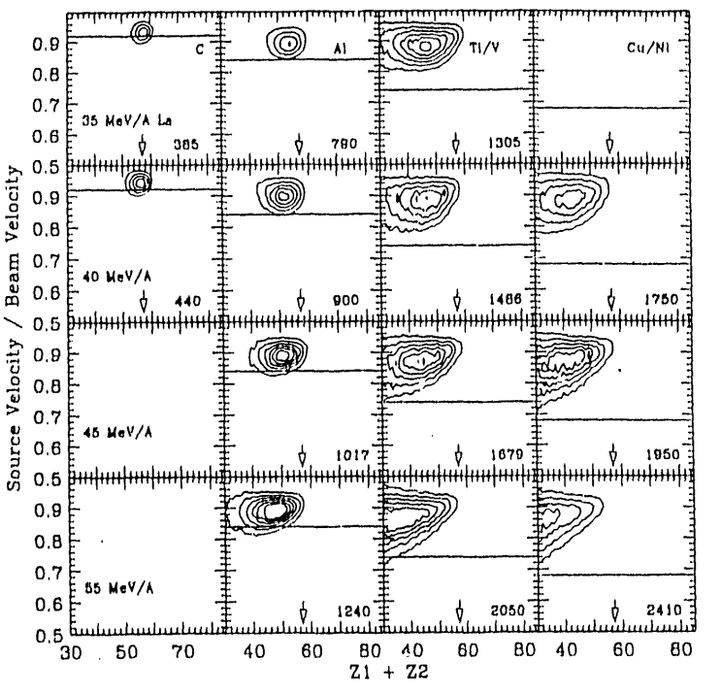

Figure II.C. 2: Source velocity distributions as a function of total charge for events in which two complex fragments were detected

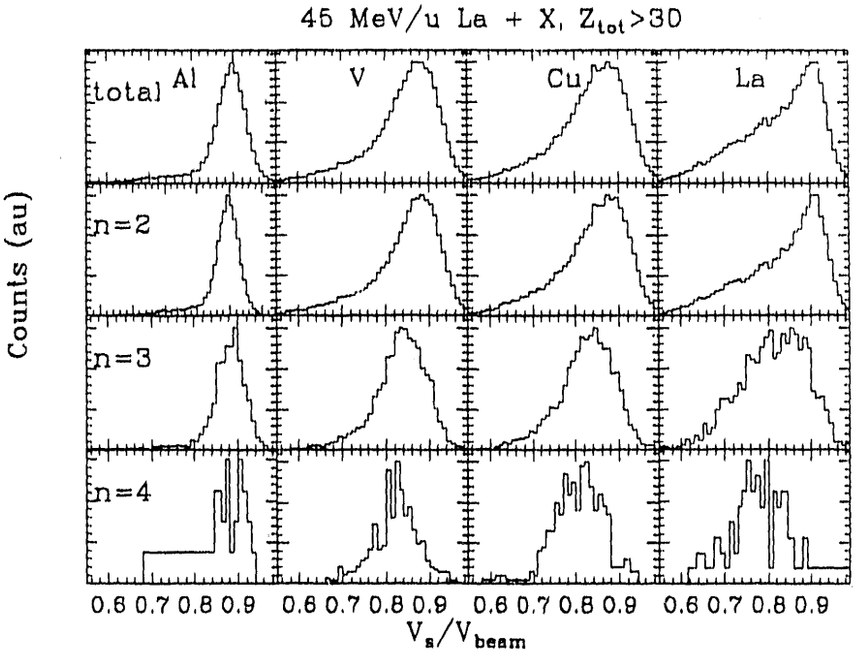

Figure II.C. 3: Source velocity distributions for reactions at E/A=45 MeV in which 2, 3, or 4 complex fragments were detected.

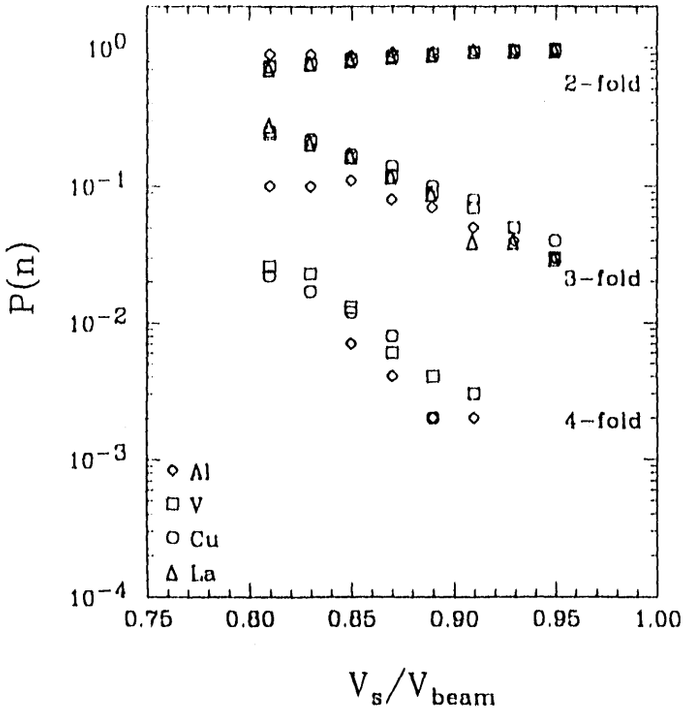

Figure II.C. 4: Probability of decay by n-complex fragments as a function of source velocity for reactions at E/A=45 MeV.

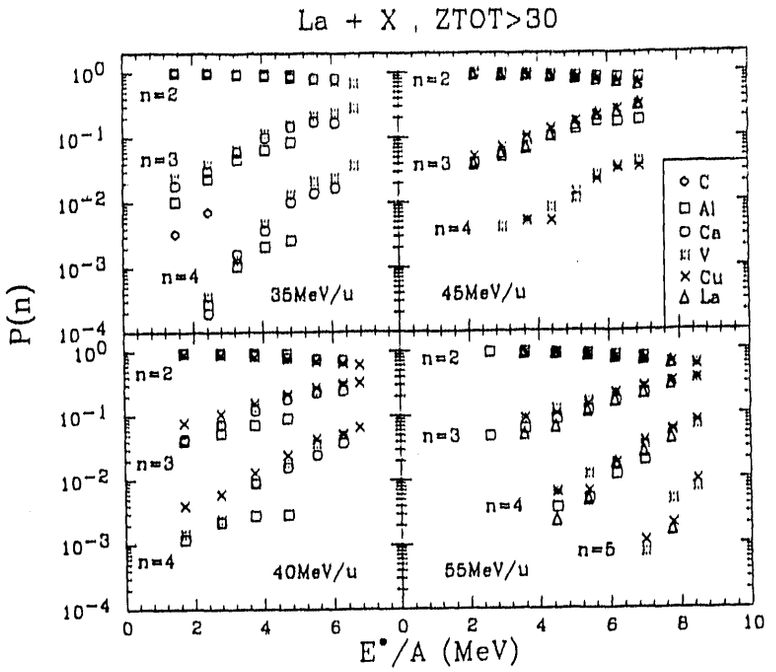

Figure II.C. 5: Probability of decay by n-complex fragments as a function of excitation energy per nucleon for all systems and energies studied.

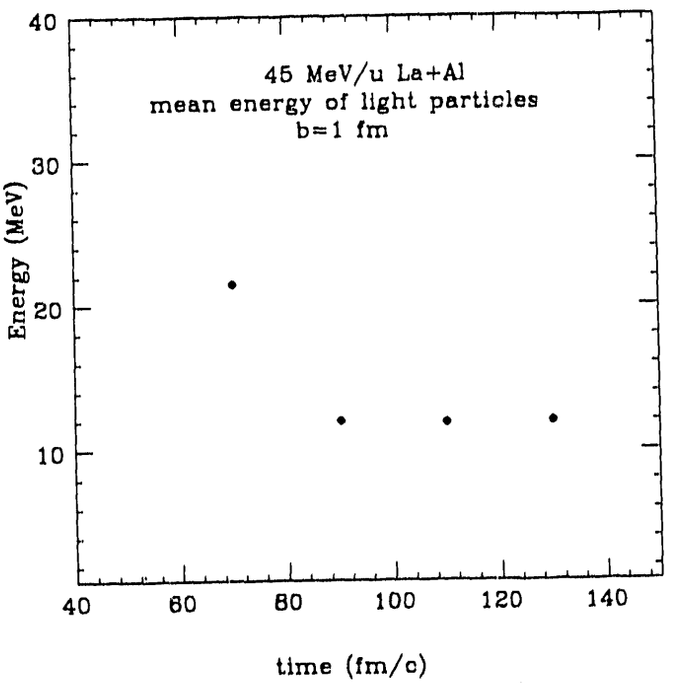

Figure II.C. 6: Mean energy of emitted light particles as a function of time for the reaction La+Al at E/A=45 MeV and b=1 fm simulated by the Landau-Vlasov equation.

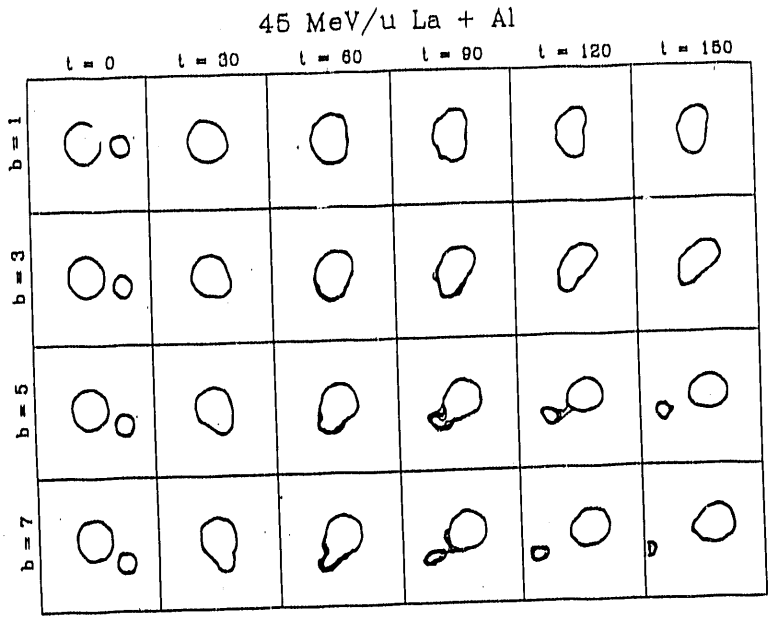

Figure II.C. 7: Dynamical evolution in space of the reaction La+Al at E/A=45 MeV for various impact parameters.

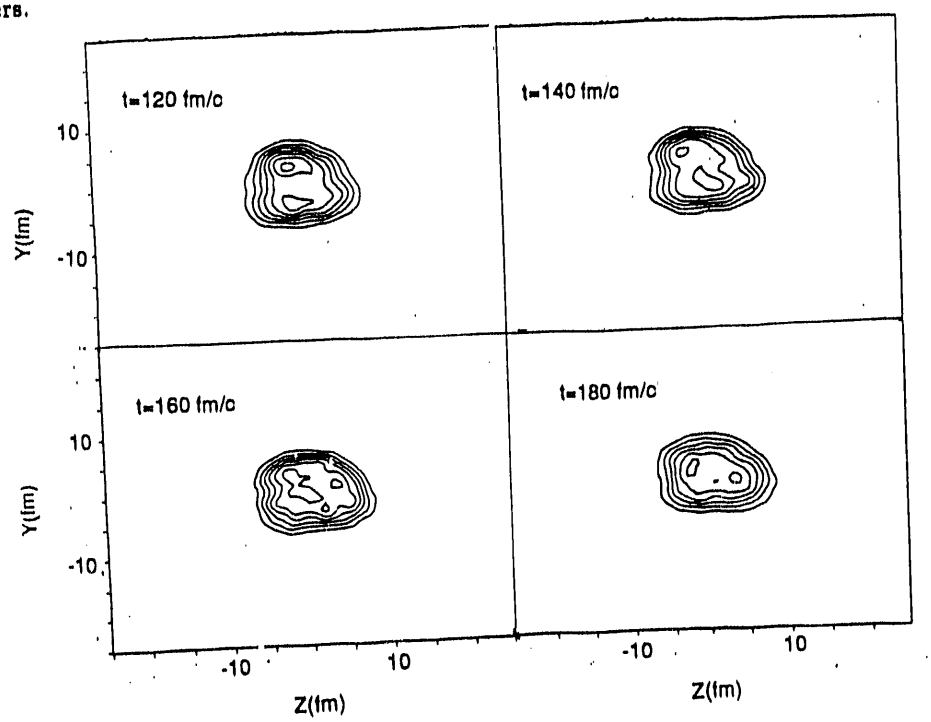

Figure II.C. 8: Density plots of the nucleons in space at various times for La + Al at E/A=45 MeV and b=3 fm. Z is the beam direction,Y is the out-of-plane direction.

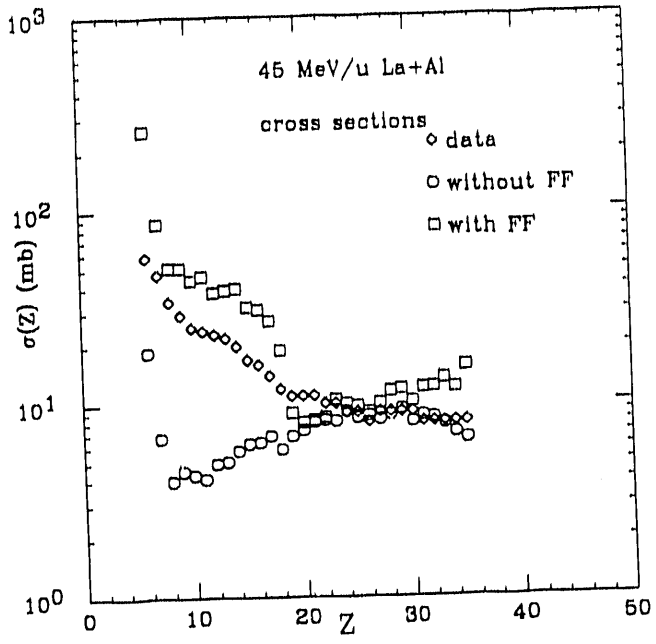

Figure II.C. 9: Cross sections for the reaction La+Al at E/A=45 MeV determined experimentally (diamonds) and simulated without fast-fission (circles) and with fast-fission (squares).

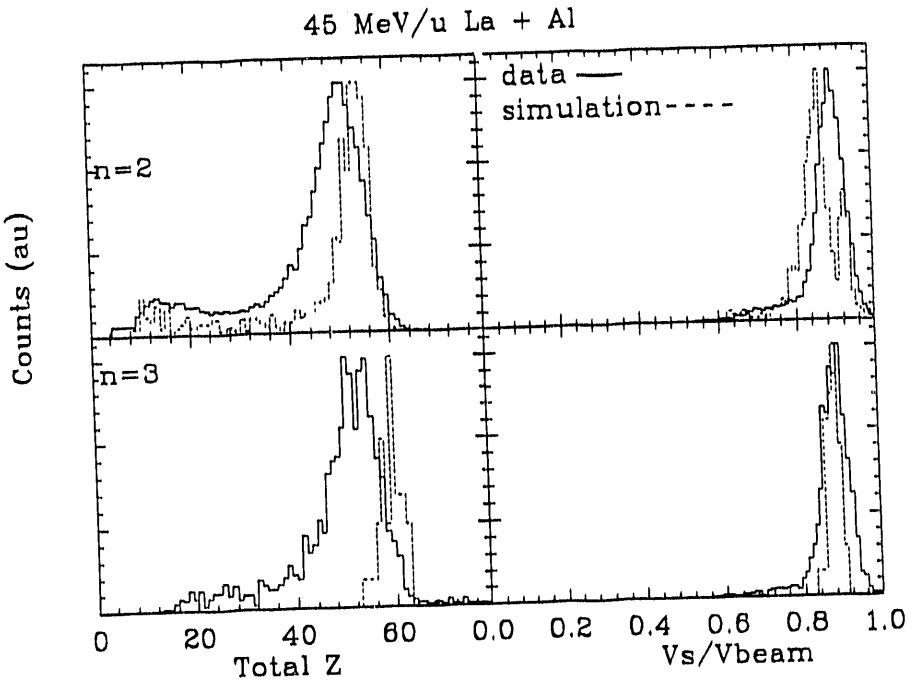

Figure II.C. 10: Experimental (solid line) and model (dashed line) total charge and source velocity distributions for events with 2 and 3 complex fragments detected for the reaction La+Al at E/A=45 MeV.

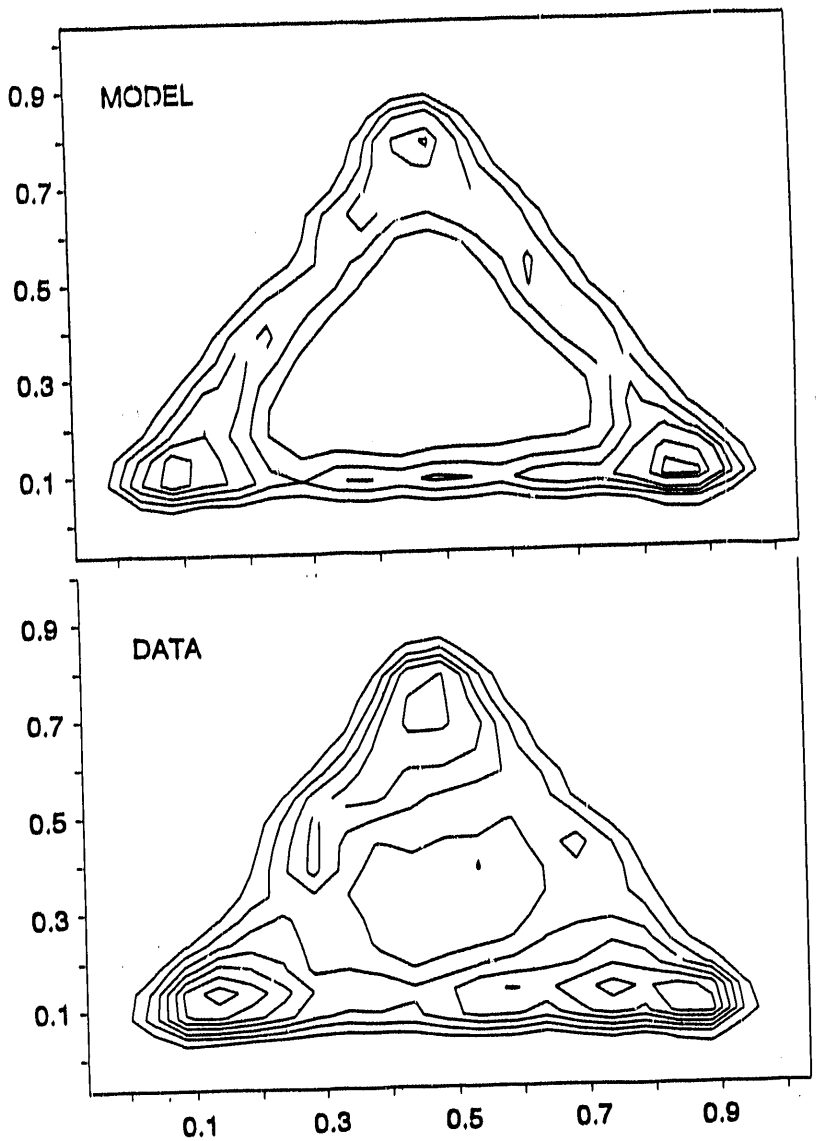

Figure II.C. 11: Experimental (bottom) and model (top) Dalitz-like plots for the reaction La+Al at E/A=45 MeV.

II.D The Maryland Very Forward Array

J. Y. Shea and A. C. Mignerey

The Maryland Very Forward Array is to be used in conjunction with the Michigan State University (MSU) 4π Array[1] for the study of peripheral intermediate-energy heavy-ion collisions. We plan to study ^{129}Xe-induced reactions at E/A = 40 - 60 MeV using the MSU National Superconducting Cyclotron. The low angle coverage of the Maryland Very Forward Array will provide for detection of heavy projectile-like fragments, normally missed by the MSU 4π Array.

The Maryland Very Forward Array is schematically shown in Fig. II.D-1. It consists of an annular Si detector backed by a plastic phoswich array. The Si detector, manufactured by Micron, has a thickness of 300 μm, an active inner diameter of 4.8 cm, and an outer diameter of 9.6 cm. The Si ring is segmented into 16 sectors on the back side and 16 small concentric rings on the front (not shown in Fig. II.D-1). The plastic phoswich array consists of 16 individual phoswich detectors. Each of the phoswich detectors is made of a 1-mm thick fast plastic scintillator glued to a 10-cm thick slow plastic scintillator. The photomultiplier tube is optically coupled to the scintillator through a light guide, and the scintillation light is collected by a photomultiplier tube. The 16 phoswich detectors are assembled in a cone-like geometry. The front side of the cone overlaps with the back of the Si ring. A side view of the detector system is shown in Fig. II.D-2. The front of the Si detector is designed to be positioned at a distance of 62 cm from the target inside the MSU 4π Array. The entire array covers an azimuthal angular range of 2.2° to 4.4°.

If a particle passes through the Si and stops in the fast plastic, then the combination of the Si and the fast plastic provides a ΔE-E measurement for particle identification. If the particle has enough energy to punch through both the Si and the fast plastic, and if it stops in the slow plastic, the phoswich technique[2] will be used for particle identification. An energy loss calculation provides a rough estimate of the energy threshold and the detector dynamic range for representative product nuclides. Considering the proposed ^{129}Xe-induced reactions at E/A = 50 MeV, we estimated the detector dynamic range for 9 different ions species. The results are listed in Table II.D-1. For a given energy range, the reaction products could stop (S), pass through (Y), or not trigger (N) the Si, the fast plastic, or the slow plastic detector. Table II.D-1 shows that for the heavier fragments with charges near the projectile's (Z = 54), particle identification can be achieved by using the Si-fast plastic combination to measure the ΔE-E of the fragments because they will be stopped in the fast

plastic, even at the projectile energy. For the lighter products ($Z \leq 40$) the plastic phoswich will be needed. For example, if the energy per nucleon (E/A) of a ^{65}Zn ($Z = 30$) fragment is above 45 MeV, the fragment will punch through both the Si and the fast plastic and stop in the slow plastic, then the plastic phoswich should be used for particle identification; if the E/A of the ^{65}Zn fragment is between 22 and 45 MeV, the fragment will not reach the slow plastic scintillator, and then the Si-fast plastic combination will provide the ΔE-E measurement for particle identification. For light ions such as protons and alpha particles, the plastic phoswich will be used for particle identification over a large energy range (E/A = 11-121 MeV). Any protons or alpha particles with more than E/A = 121 MeV kinetic energy will punch through the entire length of the detector array and can not be identified directly (although some information will be available from the punch through energy). The upper energy limit is not given for the ions with $Z \geq 10$ since they will be stopped in the slow plastic scintillator even at E/A = 50 MeV. For the less energetic particles which stop in the Si detector neither the ΔE-E nor the phoswich can be used for particle identification. Therefore, the upper limit for the lowest energy range for each ion species shown in Table II.D-1 is the energy threshold of the detector array, unless a time-of-flight measurement becomes feasible.

REFERENCES

1.- G. D. Westfall *et al.*, Nucl. Inst. and Meth. in Phys. Res., **A238**, 347 (1985).

2.- D. H. Wilkinson, Rev. Sci. Instr. **23**, 414 (1952)

Table II.D-1 Detector Dynamic Range

	E = E /A (MeV)	Si	Fast Plastic	Slow Plastic
Z = 54 (^{129}Xe)	$24 < E \leq 54$	Y	S	N
	$E = 50$	Y	S	N
	$0 < E \leq 24$	S	N	N
Z = 50 (^{119}Sn)	$24 < E \leq 53$	Y	S	N
	$E = 50$	Y	S	N
	$0 < E \leq 24$	S	N	N
Z = 40 (^{91}Zr)	$49 < E, E = 50$	Y	Y	S
	$23 < E \leq 49$	Y	S	N
	$0 < E \leq 23$	S	N	N
Z = 30 (^{65}Zn)	$45 < E, E = 50$	Y	Y	S
	$22 < E \leq 45$	Y	S	N
	$0 < E \leq 22$	S	N	N
Z = 20 (^{40}Ca)	$39 < E, E = 50$	Y	Y	S
	$19 < E \leq 39$	Y	S	N
	$0 < E \leq 19$	S	N	N
Z = 10 (^{20}Ne)	$27 < E, E = 50$	Y	Y	S
	$14 < E \leq 27$	Y	S	N
	$0 < E \leq 14$	S	N	N
Z = 6 (^{12}C)	$22 < E \leq 227$	Y	Y	S
	$11 < E \leq 22$	Y	S	N
	$0 < E \leq 11$	S	N	N
Z = 2 (^{4}He, α)	$11 < E \leq 121$	Y	Y	S
	$6 < E \leq 11$	Y	S	N
	$0 < E \leq 6$	S	N	N
Z = 1 (^{1}H, p)	$11 < E \leq 121$	Y	Y	S
	$6 < E \leq 11$	Y	S	N
	$0 < E \leq 6$	S	N	N

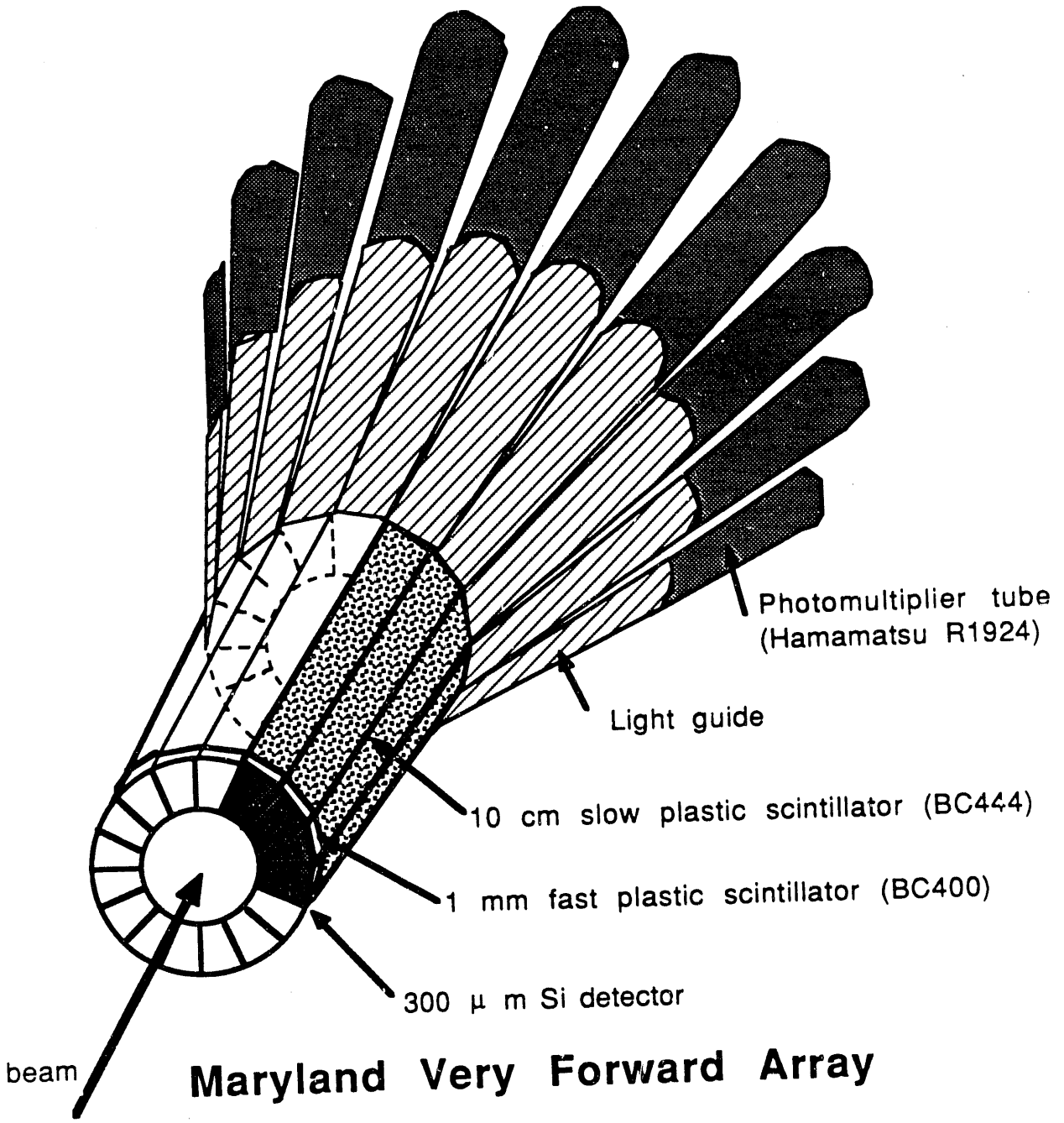

Figure II.D-1 Overview of the Maryland Very Forward Array. It consists of an annular Si detector plus sixteen identical individual plastic phoswich detectors. The system is cylindrically symmetric, and the beam is along the axis of symmetry.

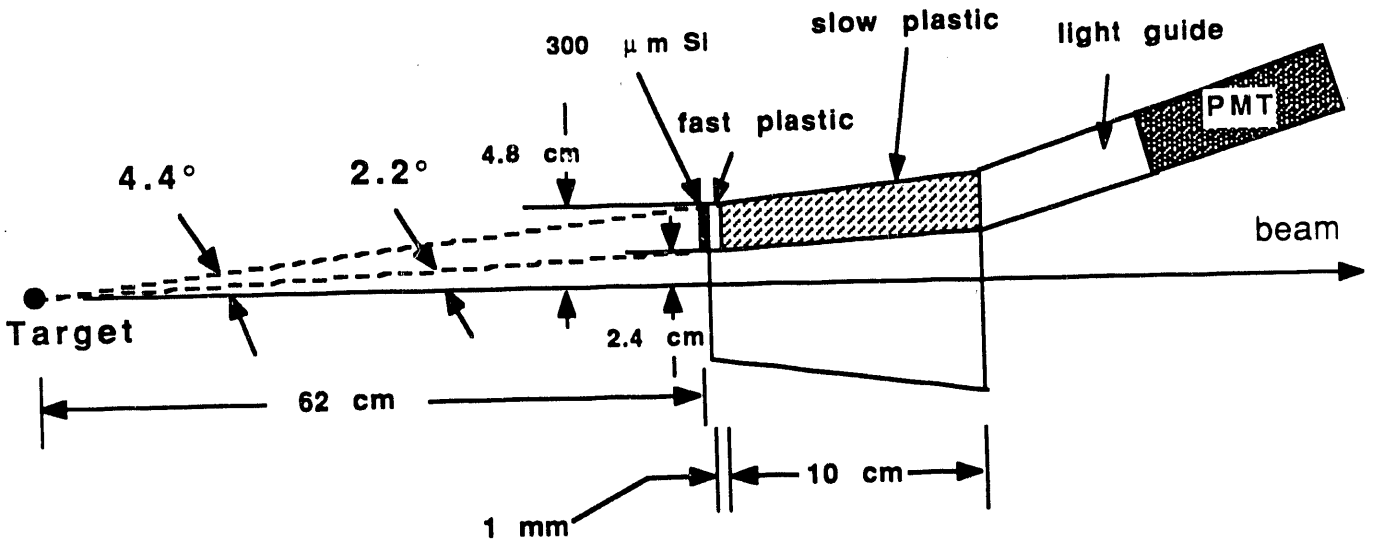

Figure II.D-2 Side view of the Maryland Very Forward Array. The front face of the detector array is positioned at a distance of 62 cm from the target. The cone-like detector array provides an azimuthal angular coverage from 2.2° to 4.4°.

III. Personnel

Faculty

Alice C. Mignerey, Professor of Chemistry

Postdoctoral Research Associate

Jing Y. Shea

Graduate Students

Alfredo Marchetti

Houria Madani

Bruce Libby

Edmundo Garcia-Solis

Daniel Russ

IV. Publications 1990-1991

A. Articles in Refereed Journals

1. Heat Partition in the E/A = 8.5 EeV $^{74}Ge + ^{165}Ho$ Reaction, K.Kwiatkowski, R. Planeta, S. H. Zhou, V. E. Viola, H. Breuer, M. A. McMahan, and A. C. Mignerey, Phys. Rev. C **41** (1990) 958-972.

2. Nucleon Exchange Properties of the E/A = 8.5 MeV $^{74}Ge + ^{165}Ho$ Reaction, R. Plantea, K. Kwiatkowski, S. H. Zhou, V. E. Viola, H. Breuer, M. A. McMahan, W. Kehoe, and A. C. Mignerey, Phys. Rev. C **41** (1990) 942-957.

3. Equilibrium and Non-Equilibrium Complex Fragment Emission in 50-100 MeV/u $^{139}La + ^{12}C$ Reactions, D.R. Bowman, G.F. Peaslee, N. Colonna, R.J. Charity, M.A. MaMahan, D. Delis, H. Han, K. Jing, G.J. Wozniak, L.G. Moretto, W.L. Kehoe, B. Libby, A.C. Mignerey, A. Moroni, S. Angius, I. Iori, A. Pantaleo, and G. Guarino, Nuclear Phys. **A523** (1991) 386-425.

4. Multifragment Events from Heavy Ion Collisions: Sources and Excitation Functions, Y. Blumenfeld, N. Colonna, P. Roussel, D.N. Delis, K. Hanold, J.C. Meng, G.F. Peaslee, G.J. Wozniak, L.G. Moretto, B. Libby, A.C. Mignerey, G. Guarino, N. Santoruvo, and I. Iori, Phys. Rev. Lett. **66** (1991) 576-579.

5. A Modular Array to Detect Complex Fragments Produced in Intermediate-Energy Reverse-Kinematics Reactions, W.L. Kehoe, A.C. Mignerey, A. Moroni, I. Iori, G.F. Peaslee, N. Colonna, K. Hanold, D.R. Bowman, L.G. Moretto, M.A. McMahan, J.T. Walton and G.J. Wozniak, Nuclear Instruments and Methods in Physics Research **A311** (1992) 258.

B. Conference Proceedings

1. The Search for Multifragmentation, A.C. Mignerey, W.L. Kehoe, A. Marchetti, S. Bradley, D.R. Bowman, R.J. Charity, H. Han, K. Jing, R.J. McDonald, M.A. McMahan, L.G. Moretto, L. Vinet, G.J. Wozniak, I. Iori, and A. Moroni, Workshop on Nuclear Dynamics VI, Jackson Hole, Wyoming, February 17-24, 1990, LBL-28709, p. 155.

2. Mass and Charge Distributions in Strongly Damped Heavy-Ion Reactions, H. Madani, A.A. Marchetti and A.C. Mignerey, Proceeding of the 7th Winter Workshop on Nuclear Dynamics: Advances in Nuclear Dynamics, Key West, Florida, U.S.A., January 26 - February 2, 1991,World Scientific, 1991, p. 86.

3. Sources and Characteristics of Complex Fragments in La-Induced Reactions, P. Roussel-Chomaz, Y. Blumenfeld, R. Charity, M. Colonna, N. Colonna, B. Libby, K. Hanold, L. Moretto, G. Peaslee, and G. Wozniak, Proceedings of the XIV Annual Symposium on Nuclear Physics, Cuernavaca, Mexico, January 7-10, 1991.

4. Excitation Functions for Multifragment Decay in La-Induced Reactions, L. Moretto, P. Roussel-Chomaz, Y. Blumenfeld, R. Charity, M. Colonna, N. Colonna, B. Libby, K. Hanold, G. Peaslee and G.J. Wozniak, Proceedings of the XXIX International Winter Meeting on Nuclear Physics, Bormio, Italy, January 14-18, 1991.

C. Published Abstracts

1. Target Dependence of Complex Fragment Production in La-Induced Reactions at E/A = 47 MeV, A.C. Mignerey, W.L. Kehoe, A. Marchetti, D.R. Bowman, R.J. Charity, H.Han, K. Jing, R.J. McDonald, M.A. McMahan, L. Vinet, G.J. Wozniak, L.G. Moretto, A. Moroni, I. Iori, and S. Bradley, BAPS **35**, 998 (1990).

2. Nuclear Chemistry for Non-Traditional Audiances, G.E. Gordon and A.C. Mignerey, 200th ACS National Meeting, Division of Nuclear Chemistry and Technology, paper #35, Washington D.C. (1990).

3. Decay of Hot Nuclei Formed in La-Induced Reactions at E/A = 45 MeV, B. Libby, A.C. Mignerey, L.G. Moretto, G.F. Peaslee, P. Roussel-Chomaz, X. Sui, G.J. Wozniak and S. Bradley, BAPS **36** (1991) 1243.

4. Comparison of Projectile-Like Fragmant Mass and Charge Distributions with Nucleon Exchange Model Predictions for ^{56}Fe-Induced Reactions Between 8.5 and 15 MeV/u, H. Madani, A.C. Mignerey, A.P. Weston-Dawkes, A.A. Marchetti, W.L. Kehoe and F.E. Obenshain, BAPS **36** (1991) 1271.

5. Mass and Charge Distributions and Nucleon Exchange Model Predictions for ^{35,37}Cl-Induced Reactions, A.A. Marchetti, A.C. Mignerey, H. Madani, K. Morley, B. Libby, W.L. Kehoe, H. Breuer, F.E. Obenshain and K. Wolf, BAPS **36** (1991) 1272.

6. Study of the Decay of Hot Nuclear Systems Formed in La-Induced Reactions at E/A = 45 and 55 MeV, B. Libby, H. Madani, A.A. Marchetti, A.C. Mignerey, P. Roussel-Chomez, N. Colonna, Y. Blumenfeld, D. Delis, M.A. McMahan, J.C. Meng, L.G. Moretto, G.F. Peaslee, Q.C. Sui, G.J. Wozniak and S. Bradley, BAPS **36** (1991).

V. Acknowledgments

I wish to thank the U. S. Department of Energy, Division of Nuclear Physics of the Office of High Energy and Nuclear Physics for supporting the program of research summarized in this report. The Experimental Nuclear Physics Group here at the University of Maryland has provided the majority of the support for the VAX computer system used in the analysis of experimental data and for the PACE calculations and the nucleon exchange model calculations. Support of the University of Maryland Computer Science Center is also gratefully acknowledged.

The Bevalac program would not have been possible without the strong involvement of our collaborators in the Moretto-Wozniak Group at Lawrence Berkeley Laboratory. A major portion of the detectors and electronics come under their jurisdiction. As always, the untiring efforts of Jose Alonso, Bob Stevenson, Peggy McMahan, Fred Lothrop and the rest of the Bevalac staff are greatly appreciated.

I would also like to acknowledge the contributions of our MSU collaborators, in particular Gary Westfall, Skip Vander Molen and Len Morris, during discussions on the design of the Very Forward Array.

END

DATE
FILMED
4/9/92